Clinical Immunology 284 (2026) 110676

Contents lists available at ScienceDirect

Clinical Immunology

journal homepage: www.elsevier.com/locate/yclim

HIV patients with poor immune recovery show exhausted CD4$^+$ stem cell memory cells and impaired COVID-19 vaccine response

Susanna Scaglioni [a,b,1], Andrea Lombardi [c,d,e,1,*], Giacomo M. Butta [a,b,2], Giorgio Bozzi [c], Matteo Centazzo [a,b], Bianca Mariani [c], Antonio Muscatello [c], Patrizia Bono [f], Lorena Donnici [a], Matteo Conti [a], Riccardo Nodari [a,b], Annapaola Callegaro [f], Edoardo Scarpa [a,g], Renata Grifantini [a,h], Sergio Abrignani [a,i], Raffaele De Francesco [a,b], Andrea Gori [j,k], Alessandra Bandera [c,d,e,3], Lara Manganaro [a,b,l,3,*]

[a] INGM, Istituto Nazionale Genetica Molecolare "Romeo ed Enrica Invernizzi", Milan, Italy
[b] Department of Pharmacological and Biomolecular Sciences (DISFEB), University of Milan, Milan, Italy
[c] Infectious Diseases Unit, Foundation IRCCS Ca' Granda Ospedale Maggiore Policlinico, Milan, Italy
[d] Department of Pathophysiology and Transplantation, University of Milan, Milan, Italy
[e] Centre for Multidisciplinary Research in Health Science (MACH), University of Milano, Milan 20122, Italy
[f] Microbiology and Virology Unit, Foundation IRCCS Ca' Granda Ospedale Maggiore Policlinico, Milan, Italy
[g] Department of Pharmacological Sciences, University of Milan, Milan, Italy
[h] CheckmAb Srl, Milan, Italy
[i] Department of Clinical Sciences and Community Health, University of Milan, Milan, Italy
[j] Division of Infectious Diseases, Luigi Sacco Hospital, University of Milan, Milan, Italy
[k] Department of Biomedical and Clinical Sciences, University of Milan, Milan, Italy
[l] Department of Microbiology, Icahn School of Medicine at Mount Sinai, New York, NY 10029, USA

ARTICLE INFO

Keywords:
Stem cell-like memory T cells
People with HIV (PWHIV)
Vaccine-induced immune response
Incomplete immune reconstitution

ABSTRACT

Vaccination triggers both humoral and cellular immune responses, generating memory T cells that ensure long-term protection. Among these, stem cell-like memory T cells (T_{SCM}) are crucial for durable immunity due to their self-renewal and multipotency. In people with HIV (PWHIV), vaccine-induced responses can be weakened by persistent immune dysfunction. In this study, we longitudinally analyzed T cell memory responses following mRNA-1273 vaccination in PWHIV. Individuals with incomplete immune reconstitution (CD4$^+$ < 500 cells/μL, CD4/CD8 < 0.4) showed reduced frequencies of Spike-specific CD4$^+$ T_{SCM}, lower levels of TCF-1 and higher expression of immune checkpoint molecules. We identified a subset of PD-1$^+$TIGIT$^+$ CD4$^+$ T_{SCM} and T_{CM} cells that phenotypically resemble CD8$^+$ exhausted-like progenitors (T_{PEX}) and are enriched in PWHIV with poor immune recovery. Modulation of the Wnt/mTORs pathway via GSK3β inhibition restored TCF-1 expression and partially rescued antigen responsiveness, highlighting a potential strategy to improve vaccine efficacy in PWHIV.

1. Introduction

Vaccination induces both humoral and cellular immune responses, enabling rapid and effective pathogen control upon subsequent exposure through the generation of long-lived immunological memory. Among memory T cells, stem cell-like memory T cells (T_{SCM}) are crucial for durable immunity due to their longevity, self-renewal, multipotency, and strong recall capacity [1–4]. These cells sustain long-term protection and are capable of differentiating into more mature memory subsets upon antigen re-exposure. T_{SCM} cells have been linked to the persistence of vaccine-induced immunity, as shown following yellow fever virus (YFV) vaccination [3]. Conversely, reduced T_{SCM} frequencies have been

* Corresponding authors.
E-mail address: lara.manganaro@unimi.it (L. Manganaro).
[1] Co-first authors.
[2] Current affiliation: Department of Microbiology, Icahn School of Medicine at Mount Sinai, New York, NY USA and Center for Vaccine Research and Pandemic Preparedness, Icahn School of Medicine at Mount Sinai, New York, NY, USA.
[3] Co-last authors.

https://doi.org/10.1016/j.clim.2026.110676
Received 17 October 2025; Received in revised form 11 January 2026; Accepted 29 January 2026
Available online 2 February 2026

reported in hepatitis B vaccine non-responders [5]. SARS-CoV-2 mRNA vaccines, including BNT162b2, also elicit T_{SCM} cells, suggesting a role in maintaining long-lasting immunity [1,2].

In people with HIV (PWHIV), vaccine responses are frequently diminished. Despite viral suppression with antiretroviral therapy (ART), HIV infection causes persistent immune dysfunction characterized by chronic inflammation, reduced $CD4^+$ T cell counts, and impaired B and T cell responses [6,7]. These immune alterations contribute to suboptimal vaccine efficacy, reflected in reduced seroconversion rates and the need for additional doses to reach protective antibody levels. This has been observed with vaccines for hepatitis A (HAV), hepatitis B (HBV), and monkeypox (MPXV) [8–10]. Similarly, PWHIV with low $CD4^+$ T cell count and low CD4/CD8 ratio display reduced immune response following YFV vaccination, reduced long-term B cell memory following HPV vaccination and defective antibody production after the 2009 H1N1 influenza vaccine [11–13].

During the COVID-19 pandemic, vaccination in PWHIV became a priority due to their increased risk for severe disease [14,15]. COVID-19 vaccines have shown favorable safety and immunogenicity in PWHIV with high $CD4^+$ T cell counts (>500 cells/μL), with immune responses comparable to HIV-negative individuals. However, those with $CD4^+$ T cell counts below 200 cells/μL exhibit significantly reduced seroconversion rates and lower neutralizing antibody titers [16–20]. Similar trends have been observed for T cell responses, which are generally preserved in individuals with higher $CD4^+$ counts but impaired in those with advanced immune deficiency. A higher incidence of breakthrough infections in PWHIV with low $CD4^+$ T cell counts raises concerns about the durability of vaccine-induced protection [21,22].

HIV-induced chronic immune activation leads to T cell exhaustion, with increased expression of activation and inhibitory receptors on both $CD4^+$ and $CD8^+$ T cells [7,23–28]. This results in a reduction of naïve and central memory T cells (T_{CM}) and expansion of more differentiated or exhausted phenotypes [29–31]. Despite this, the effect of HIV on T_{SCM} cells remains insufficiently characterized.

In this study, by taking advantage of longitudinal sampling during the COVID-19 vaccination campaign, we examined the generation of vaccine-specific T_{SCM} cells and the T memory phenotype in PWHIV. We observed a reduction in Spike-specific $CD4^+$ T_{SCM} cells in individuals with incomplete immune reconstitution ($CD4^+$ T cells <500 cells/μL, CD4/CD8 ratio < 0.4), accompanied by higher expression of PD-1 and TIGIT on $CD4^+$ T_{SCM} and T_{CM} cells. We also identified a novel subset of $CD4^+$ T_{SCM} and T_{CM} co-expressing PD-1 and TIGIT, resembling $CD8^+$ progenitors predisposed to exhaustion ($CD8^+$ T_{PEX}) [32–34]. These cells were enriched in PWHIV with poor immune recovery. Furthermore, reduced expression of TCF-1, a transcription factor essential for T cell homeostasis, was observed across T cell subsets, and its restoration via GSK3β inhibition partially rescued the response of $CD4^+$ T_{SCM} cells to SARS-CoV-2 Spike peptides at six months post-booster.

2. Methods

2.1. Study design

The study included PWHIV on stable ART and healthy donors (HDs), all vaccinated with three doses of the mRNA-1273 vaccine. PWHIV were enrolled from the Infectious Diseases Unit, IRCCS Ospedale Maggiore Policlinico, Milan, Italy. HDs were healthcare workers without chronic conditions or immunosuppressive treatment, vaccinated during the same period. At baseline (T0), participants completed a questionnaire on demographic and clinical data and were monitored for SARS-CoV-2 infection at each time point. Only COVID-19-naïve individuals (anti-N negative throughout the study) were included. PWHIV maintained routine clinical follow-up. Detailed participant characteristics are shown in Table 2.

2.2. Sex as a biological variable

Our study involved male and female subjects. Sex was not considered as a biological variable.

2.3. Blood samples collection, processing, and storage

Blood was collected at five time points: before vaccination (T0), 28 days post-second dose (T1), 5 months post-second dose (T2), 28 days post-third dose (T3), and 6 months post-third dose (T4) (see Fig. 1A). PBMCs were isolated via density gradient centrifugation (SepMate™/Lymphoprep™STEMCELL Technologies), then cryopreserved in heat-inactivated fetal bovine serum (FBS, Gibco) with 10% DMSO. Sera were obtained by centrifugation in serum separator tubes (525 *g*) and stored at −20 °C.

2.4. ANTI-S and ANTI-N antibody titers measurement

Elecsys anti-SARS-CoV-2 and Elecsys anti-SARS-CoV-2 S kits (Roche Diagnostics) were used on Roche Cobas e801 (Roche Diagnostics) to measure serum anti-Spike RBD (total Ig) and anti-Nucleocapsid antibody titers, respectively.

2.5. Cell culture

Human embryonic kidney 293TN (HEK293TN) cell line (System Bioscience, cat#LV900A-1) was cultured in Dulbecco's Modified Eagle Medium (DMEM, Gibco) supplemented with 10% of heat-inactivated FBS, 100 U/mL penicillin, 100 μg/mL streptomycin, 2 mM L-glutamine (Euroclone), 1 mM sodium pyruvate and 1× MEM non-essential amino acids (NEAA, Gibco). Cells were maintained at 37 °C in a 5% CO2 humidified incubator. Testing for mycoplasma was carried out using MycoAlertTM Mycoplasma Detection Kit (Lonza).

HEK293TN-hACE2 cells were derived from HEK293TN after transduction with a lentiviral vector coding for human ACE2 (hACE2) gene and Hygromycin resistance as previously described (36). HEK293TN-hACE2 cells were maintained in the same culture conditions of HEK 293TN, with the addition of 250 μg/mL Hygromycin (Gibco) in the culture medium to ensure the specific propagation of transduced cells.

2.6. Production of SARS-CoV-2 VSV-Pseudotyped particles and titration

HEK293TN cells (5×10^6) were seeded in 150 mm dishes and transfected 24 h later with 12 μg of pcDNA3.1 encoding C-terminally truncated (Δ19) SARS-CoV-2 Spike variants (D614G, B.1.617.2, BA.1, or BA.5). After 24 h, cells were inoculated with VSVΔG/ffLuc/GFP seed particles (1:100 dilution in 2% FBS DMEM; kindly provided by Dr. Michael Letko, Washington State University) for 1 h at 37 °C. Cells were then washed with PBS and incubated in fresh 2% FBS DMEM. Supernatants were collected 24 h later, filtered (0.45 μm PES), and concentrated by ultracentrifugation (2 h, 80,000 ×g, SW 32Ti rotor). Viral pellets were resuspended in PBS to obtain a 400× concentrated stock, shaken for 30 min at 4 °C, and stored at −80 °C.

HEK293TN-hACE2 cells were seeded in 24-well plates at 500 cells/μL (1 mL/well). After 24 h, cells were infected with six 3-fold serial dilutions of pseudoparticles. Twenty-four hours post-infection, cells were fixed in 1% paraformaldehyde, and GFP-positive cells were quantified by flow cytometry to calculate viral titers (IFU/μL).

2.7. Neutralization assay

HEK293TN-hACE2 cells (10^4 cells/well) were seeded in white 96-well plates in 100 μL of complete DMEM. The next day, sera were serially 3-fold diluted in PBS (7 points + PBS control) and incubated with pseudoparticles (MOI 0.1) for 1 h at 37 °C. Cells were then infected in triplicate with the virus-serum mix. After 16 h, luciferase activity was

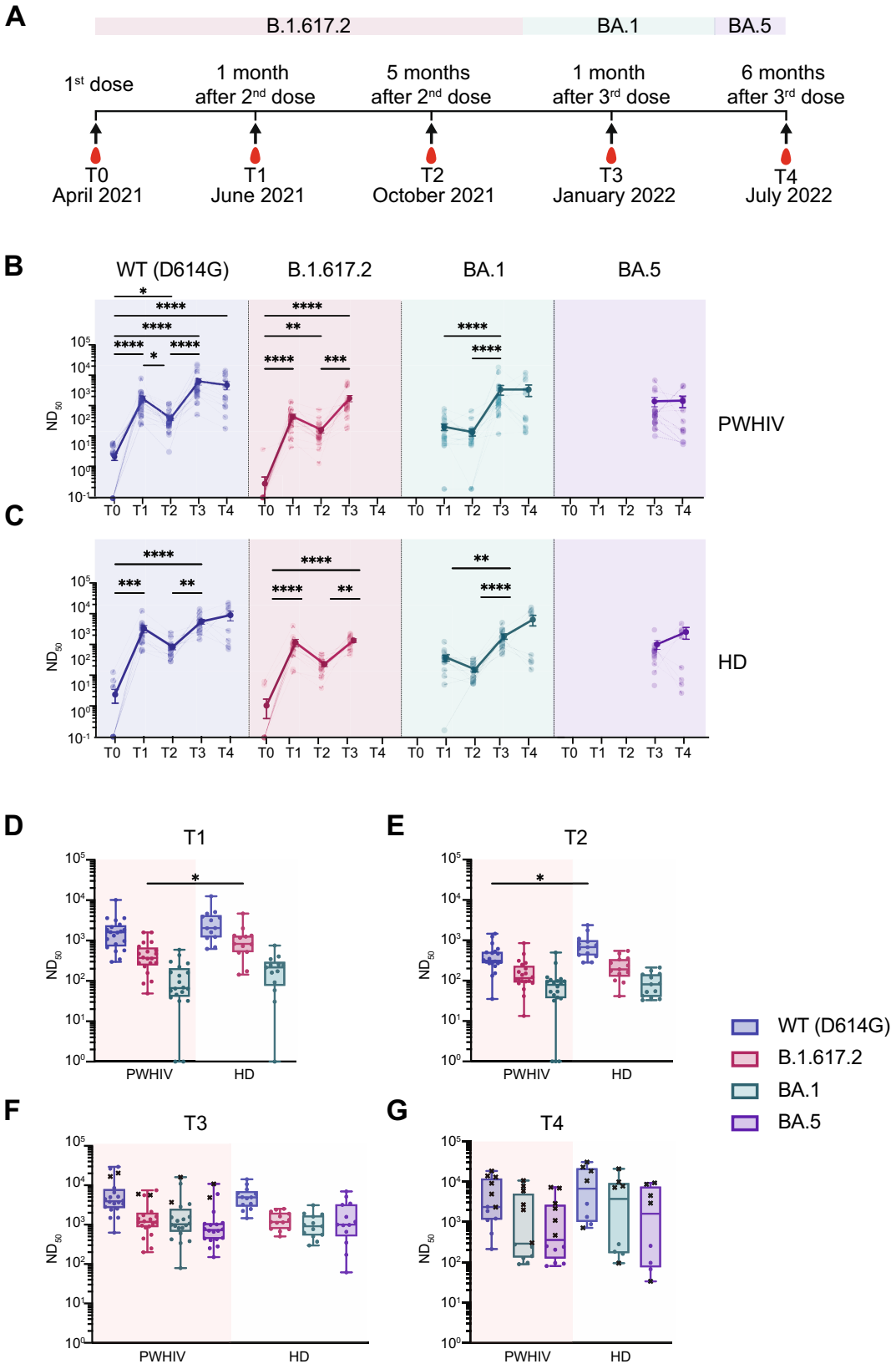

Fig. 1. Early impairment in SARS-CoV-2 Neutralizing Antibodies in PWHIV is restored by the third dose Booster, regardless $CD4^+$ T cell count.
(A) Participants received three mRNA-1273 vaccine doses. Blood samples were collected at the indicated time points. (B-C) Longitudinal monitoring of ND_{50} of sera from PWHIV ($n = 22$) (B) and HDs ($n = 14$) (C) towards SARS-CoV-2 pseudoviruses carrying the indicated variants of Spike. Individual subjects are shown as light symbols with dotted lines connecting for longitudinal samples. Averages are shown in thick lines. *P* values show statistical differences between each time point. (Friedman test $*p \leq 0.05$, $**p \leq 0.01$, $***p \leq 0.001$, $****p \leq 0.0001$). (D-G) Comparison of ND_{50} between PWHIV and HDs for the indicated SARS-CoV-2 Spike variants at T1 (D), T2 (E), T3 (F) and T4 (G). Subjects that resulted positive for anti-N are indicated with an (x). Kruskal-Wallis test was used for statistical analysis ($*p \leq 0.05$, $**p \leq 0.01$, $***p \leq 0.001$, $****p \leq 0.0001$).

measured using the Bright-Glo™ Luciferase System (Promega) and Infinite F200 plate reader (Tecan). Relative light units (RLUs) were normalized to PBS controls, and ND_{50} values were calculated by nonlinear regression using GraphPad Prism.

2.8. AIM assay and intracellular cytokine staining

Cryopreserved PBMCs were thawed and rested overnight in RPMI 1640 (Gibco) supplemented with 10% heat-inactivated FBS, 100 U/mL penicillin, 100 μg/mL streptomycin (Euroclone), 1× MEM non-essential amino acids, 2 mM L-glutamine, 1 mM sodium pyruvate, and 10 mM HEPES (Gibco). The next day, 1.5×10^6 PBMCs/well were seeded in 96 U-well plates and stimulated with 1 μg/mL PepTivator® SARS-CoV-2 Prot_S Complete (Miltenyi Biotec). Cells treated with 1 μg/mL SEB (Merck) served as positive control; untreated cells as negative control. Brefeldin A (10 μg/mL, Merck) was added 2 h post-stimulation. After 16 h, cells were collected for flow cytometry. Cells were stained with two panels of fluorochrome-conjugated antibodies to characterize $CD4^+$ (CD3 PE-Cy7, CD4 APC-fire, CD45RA APC, CCR7 BV711, CD95 BV421, CD154 PE-Cy5, TNF-α BUV395, IFN-γ PE) and $CD8^+$ (CD3 PE-Cy7, CD8 FITC, CD45RO BUV805, CCR7 BV711, CD95 BV421, CD69 APC, CD154 PE-Cy5, TNF-α BUV395, IFN-γ PE) T cell responses. After washing in PBS, cells were incubated for 20 min at 37 °C in the dark with surface antibodies and viability dye, then washed in MACS buffer (Miltenyi Biotec), and fixed/permeabilized with Cytofix/Cytoperm™ (BD Biosciences) for intracellular staining. Green fluorescent reactive dye (Thermo Fisher, panel 1), FVS780 (BD, panel 2) were used as **Viability dyes**. Samples were acquired on a BD FACSymphony™ A5 and analyzed using FlowJo (FlowJo, LLC).

2.9. Staining for checkpoint marker characterization and TCF-1

For flow cytometric analysis of TCF-1, SLAMF6, PD-1, TIGIT, and TIM-3, thawed PBMCs were rested overnight in complete RPMI. The next day, 5×10^6 cells were stained with surface antibodies targeting CD3, CD4, CD45RA/RO, CCR7, CD95, CD27, PD-1, TIGIT, TIM-3 along with FVS780 viability dye (20 min at 37 °C). After a wash, cells were incubated with FITC anti-CD352 (SLAMF6) antibody for 15 min at 4 °C. For TCF-1 and SLAMF6 detection, cells were stained for surface antibodies (CD4, CD45RA, CD45RO, CD95, CD27 and SLaMF6) along with fixable live/dead stain (FVS780) as described above and then fixed/permeabilized (Foxp3/Transcription Factor Buffer Set, eBioscience) and stained with PE anti-TCF-1 (30 min, RT). Samples were acquired on a BD FACSymphony™ A5 and analyzed using FlowJo (FlowJo, LLC).

2.10. TWS119 treatment

Cryopreserved PBMCs were thawed and rested in complete RPMI for 24 h (condition 1: Spike or CD3/CD28 stimulation) or 8 h (condition 2: TCF-1 and SLAMF6 staining). Cells (1.5×10^6/well) were treated with 7 μM TWS119 or DMSO (control) for 16 h. In condition 1, cells were stimulated with SARS-CoV-2 Spike peptides or CD3/CD28 and analyzed for intracellular cytokine expression using a specific antibody panel (PE-Cy7 anti-CD3, APC-fire anti-CD4, FITC anti-CD8, APC anti-CD45RA, BV711 anti-CCR7, BV421 anti-CD95, PE-Cy5 anti-CD154, PE anti-IFN-γ, BUV395 anti-TNF-α). In condition 2, cells were left unstimulated and stained for TCF-1 and SLAMF6 as described, including PE-Cy7 anti-CD3.

2.11. T cell activation via CD3 and CD28

Cryopreserved PBMCs were thawed and rested for 8 h in complete RPMI medium then seeded at $0{,}5*10^6$ PBMCs/well in a 96 U well plate adding DMSO or TWS119 7 μM. After 16 h of treatment, cells were stimulated with T Cell TransAct™ (Miltenyi) following manufacturer's instructions. The following panel of live/dead and antibodies was exploited: LIVE/DEAD Violet fluorescent reactive dye (Thermo Fisher Scientific), PE-Cy7 anti-CD3, APC-fire anti-CD4, PE anti-CD45RO, BV711 anti-CCR7, BV421 anti-CD95, PE-CF594 anti-PD-1, BV605 anti-TIGIT, BUV395 anti-TNF-α, FITC anti-pS6.

2.12. Study approval

All participants provided written informed consent. The study was approved by the INMI "Lazzaro Spallanzani" Ethics Committee (protocol 286_2021) and conducted in accordance with the Declaration of Helsinki and Good Clinical Practice.

Antibody	Supplier	Identifier
PE-Cy7 anti-CD3	BioLegend	300,316
APC-fire anti-CD4	BioLegend	300,560
APC anti-CD45RA	BioLegend	304,150
BV711 anti-CCR7	BD Biosciences	566,602
BV421 anti-CD95	BioLegend	305,624
PE-Cy5 anti-CD154	BioLegend	310,808
FITC anti-CD8	BioLegend	344,704
BUV805 anti-CD45RO	BD Biosciences	748,367
APC anti-CD69	BioLegend	310,909
BUV395 anti-TNF-α	BD Biosciences	563,996
PE anti-IFN-γ	BioLegend	502,509
BUV395 anti-CD4	BD Biosciences	564,724
APC-R700 anti-CD27	BD Biosciences	565,116
FITC anti-CD352	Miltenyi	130–126-006
PE anti-TCF1	BioLegend	655,207
PE-CF594 anti-PD-1	BD Biosciences	566,846
BV605 anti-TIGIT	BD Biosciences	747,841
BV480 anti-TIM3	BD Biosciences	746,771

3. Results

3.1. Study cohort

We enrolled 22 PWHIV and 14 healthy donors (HDs) for this study. All participants received three doses of the mRNA-1273 vaccine within the same time frame. At the time of enrollment, all participants were COVID-naïve, meaning their level of anti-N before vaccination ($T = 0$) was below the detection limit. The two groups were similar in age (median, 45 years), but the PWHIV group was predominantly male

Table 1
Characteristics of enrolled participants at T0.

	HD ($N = 14$)	PWHIV ($N = 22$)
Male gender, N (%)	7 (50)	18 (82)
Age, years*	45 (15)	45 (19)
HCV-Ab positive, N (%)	–	0
HBsAg positive, N (%)	–	1 (5)
CMV IgG positive, N (%)	–	13 (59)
Years since HIV infection diagnosis*	–	2 (7)
$CD4^+$ cell count at nadir, cells/μl	–	169 (209)
Viral load zenith, copies/mL*	–	46,000 (123,260)
AIDS diagnosis, N (%)	–	7 (32)
On antiretroviral therapy	–	22 (100)
INSTI, N (%)	–	18 (82)
NNRTI, N (%)	–	2 (9)
PI, N (%)	–	2 (9)
NRTIs backbone, N (%)	–	22 (100)
TDF-TAF/FTC-3TC, N (%)	–	15 (68)
ABC/FTC-3TC, N (%)	–	4 (18)
3TC-FTC, N (%)	–	3 (14)
Plasma HIV viral load, copies/mL§	–	<50
$CD4^+$ T cell count, cells/μL	–	661 (374)
<350 cells/μL	–	5 (26)
350–500 cells/μL	–	4 (18)
>500 cells/μL	–	13 (59)

Data are expressed as mean and standard deviation unless stated otherwise.
* Median and IQR.
§ All viral loads were lower than 50 RNA copies per mL of plasma except for 1 patient who had 85 copies per mL.

(Table 1). All participants tested negative for hepatitis C virus (HCV) and did not have any underlying chronic diseases or receive immunosuppressive drugs. One participant in the PWHIV group tested positive for HBsAg. The PWHIV cohort consisted of individuals who were stable on ART and had a plasma viral load of <50 copies of HIV RNA/mL at the time of vaccination, but one patient who presented with 85 copies of HIV RNA/mL. Participants in the PWHIV cohort were under routine follow-up at the Infectious Diseases Unit of the IRCCS Ospedale Maggiore Policlinico in Milan, Italy. Blood and serum samples were collected at five time points: before the first dose (T0), 28 days after the second dose (T1), five months after the second dose (T2), 28 days after the third dose (T3), and six months after the third dose (T4) (Fig. 1A). For detailed participant characteristics, refer to Table 1.

HD, healthy donors; PWHIV, people living with HIV; NRTIs, nucleoside reverse transcriptase inhibitors; InSTIs, integrase strand transfer inhibitors; NNRTIs, non-nucleoside reverse transcriptase inhibitors; PIs, protease inhibitors; HCV, hepatitis C virus; HBsAg, hepatitis B surface antigen; CMV, cytomegalovirus.

TDF-Tenofovir Disoproxil Fumarate, TAF-Tenofovir Alafenamide, FTC-Emtricitabine, 3TC-Lamivudine, ABC-Abacavir.

3.2. Early impairment in SARS-CoV-2 neutralizing antibodies in PWHIV is restored by the third dose booster, regardless CD4$^+$ T cell count

We initially assessed the levels of anti-Spike antibodies (anti-S) at time points T1, T2, and T3 post-vaccination in PWHIV and HDs. Anti-S antibodies were detected in both groups at T1, they declined at T2 and were significantly boosted after the third dose in both groups (Supp. Fig. 1A). Notably, at T1, total anti-S antibody levels were higher in HDs compared to PWHIV. However, after the booster dose, both groups exhibited comparable titers of anti-S antibodies (Supp. Fig. 1B).

We then analyzed the neutralization capacity (ND50) of sera collected from PWHIV and HDs against the wild-type strain (D614G) and three variants of concern (VoCs): B.1.617.2 (Delta), BA.1 (Omicron), BA.5 (Omicron 5) that were circulating at the time of the vaccination campaign by exploiting pseudovirus-based neutralization assays (36) (Fig. 1A). All serum samples collected at T1 showed neutralization capacity against SARS-CoV-2 D614G, which decreased at T2. The third booster dose (T3) restored the ND50. A similar trend was observed for B.1.617.2 and BA.1 in both groups (Fig. 1B and C). At T4 the neutralization of WT, BA.1 and BA.5 seems to increase or remain stable, possibly because about half of our cohort, at the latest time point, was infected with the Omicron variant without reporting the infection as detected by anti-N serum test at T4 (Supp. Fig. 1C).

Indeed, participants actively reporting cases of SARS-CoV-2 were tracked and excluded from the study. Specifically, 1 participant with a CD4$^+$ T cell count <500 and 3 participants with an optimal immune reconstitution reported a breakthrough infection.

However, some of the participants tested positive for anti-N antibodies without reporting any infection. In detail, in 3 out of 9 PWHIV with CD4$^+$ T cell count <500 (33%), 4 out of 13 PWHIV with CD4 > 500 (31%) and 5 out of 14 HDs (36%), the levels of anti-N antibodies titer were above the limit of detection after the third booster dose. Among them, two PWHIV with CD4$^+$ T cell count <500 were anti-N positive at T3, while the other participants tested positive for anti-N antibodies more than 28 days after the third dose (T3). Considering the comparable percentage of anti-N positive individuals among the participant groups and the modest number of participants, we decided to keep considering all participants in our analysis to reflect real-world experience (Table 2).

The ND50 against the WT strain was consistently higher than other variants and the ND50 towards B.1.617.2 was higher than that of BA.1 in both groups, as expected. However, after the third booster dose, the difference between B.1.617.2 and BA.1 disappeared (Supp. Fig. 1D and E).

When comparing the ND50 between the PWHIV and HD groups, we observed that at T1, the ND50 against SARS-CoV-2 WT was similar, while the ND50 against the B.1.617.2 variant was significantly lower in PWHIV compared to HDs and BA.1 was barely neutralized by both groups (Fig. 1D).

Table 2
Results of anti-N antibodies assessment among HD and PLWH.

	PWHIV CD4 < 500	PWHIV CD4 > 500	HD
Breakthrough infection, N	1	3	0
Anti-N positive test at T3	2 (9.1%)	0 (0%)	0 (0%)
Anti-N positive test after T3	1 (11%)	4 (30.7%)	5 (35.7%)
Total of Anti-N positive	3 (33.3%)	4 (30.7%)	5 (35.7%)

At T2, the ND50 decreased in both groups, as previously reported [36–39]. However, in HDs, it remained significantly higher than in PWHIV (Fig. 1E). Notably, after the third booster dose, no differences were observed for all the variants screened, highlighting the importance of the booster dose, especially in more vulnerable individuals (Fig. 1F and G). Of note, ND50 for each variant correlated with one another (Supp. Fig. 1F).

Next, we stratified the data based on CD4$^+$ T cell count (CD4$^+$ T < 500 cells/μL, CD4$^+$ T > 500 cells/μL). Of note, CD4/CD8 ratio median was higher than 1 for the group of participants with a CD4$^+$ T count >500 cells/μL, while the median of the CD4/CD8 ratio in the group with a CD4$^+$ T count <500 cells/μL was below 0.4. In addition, among PWHIV characterized by an incomplete immune reconstitution (CD4$^+$ T count <500 cells/μL and CD4/CD8 ratio < 0.4), 7 out of 9 individuals had experienced AIDS before (Supp. Fig. 2A). In both groups, the percentage of CD4$^+$ T cells remained stable throughout the study (Supp. Fig. 2B, C, D).

The ND50 for all the variants was slightly lower in PWHIV at T1 and T2, regardless of CD4$^+$ T cell count, compared to HDs. However, after the third booster dose, these differences disappeared, indicating that the third booster is essential for increasing the neutralization capacity of the serum in all three groups analyzed (Supp. Fig. 2E-H).

These data indicate that the third booster efficiently increases anti-S titers and ND50 for all the tested SARS-CoV-2 variants in HDs and PWHIV regardless of the CD4$^+$ T cell count. Nevertheless, a modest defect in the neutralizing activity of sera from PWHIV is observed after two doses of mRNA-1273 vaccine administration.

3.3. Response to SARS-CoV-2 spike peptides is comparable in total CD4$^+$ T cells isolated from PWHIV and HDs

We analyzed the specific T cell response in HD and PWHIV stratified based on their CD4$^+$ T cell count at different time points after vaccination.

To assess the CD4$^+$ T cell response towards SARS-CoV-2 Spike, we stimulated cryopreserved PBMCs collected at the indicated time points with peptide pools spanning the original strain of SARS-CoV-2 Spike. Unstimulated and Staphylococcal Enterotoxin B (SEB)-stimulated PBMCs were used as negative and positive controls, respectively. First, we evaluated the percentage of CD4$^+$ T antigen-induced activation marker-positive (AIM$^+$) cells (CD69$^+$ and CD40L$^+$) after stimulation with SARS-CoV-2 Spike peptides (Fig. 2A). All subjects showed Spike-specific CD4$^+$ T cells one month after the second dose of the mRNA-1273 vaccine, but these declined after six months. A third booster dose restored the percentage of AIM$^+$ CD4$^+$ T cells, which again declined at T2 (Fig. 2B). When comparing the percentage of AIM$^+$ CD4$^+$ T cells among the three groups, we observed that at T1, T2, and T3 time points, PWHIV with CD4 < 500 CD4$^+$ T cells/μL had a slightly higher percentage of AIM$^+$ CD4$^+$ T cells compared to the other two groups without reaching statistical significance (Fig. 2C).

Next, we measured the SARS-CoV-2 Spike-specific CD4$^+$ T cell responses by quantifying IFN-gamma (IFN-γ) and tumor necrosis factor-

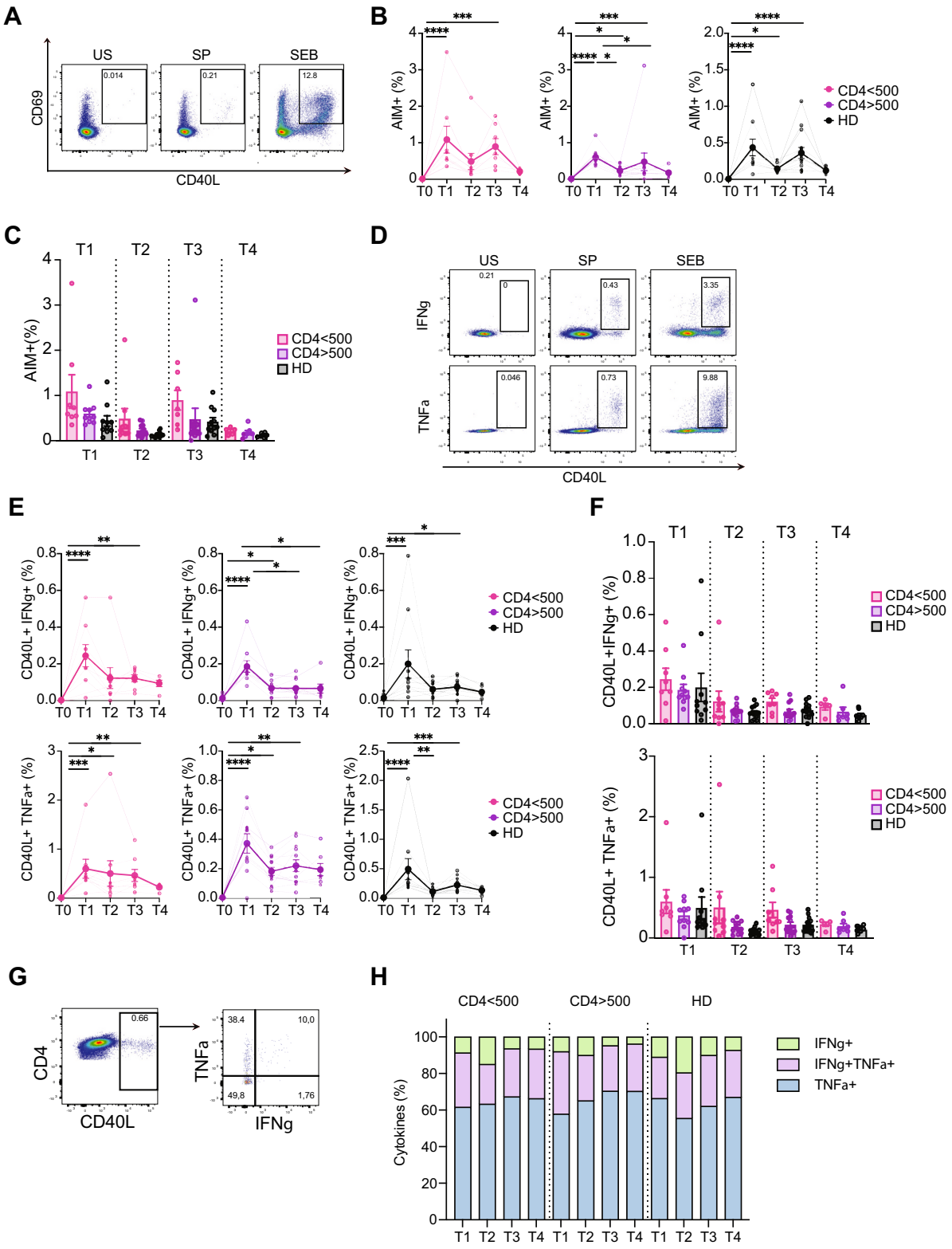

Fig. 2. Response to SARS-CoV-2 Spike peptides is comparable in total CD4$^+$ T cells isolated from PWHIV and HDs.
(A) Representative flow cytometry plots showing AIM$^+$ (CD40L$^+$CD69$^+$) CD4$^+$ T cells after Spike peptide (SP), or SEB stimulation, unstimulated (US) were used as a control. (B) Longitudinal AIM$^+$ CD4$^+$ T cell responses in PWHIV with <500 (pink), >500 CD4$^+$/μL (purple), and HDs (black). (C) AIM$^+$ CD4$^+$ T cell frequencies compared across groups at different time points. (D) Representative plots for cytokine-producing CD40L$^+$ CD4$^+$ T cells (TNF-α$^+$ and IFN-γ$^+$). (E) Longitudinal monitoring of cytokine-producing CD4$^+$ T cells post-vaccination. (F) Group comparison of frequencies of CD4$^+$ T cells CD40L$^+$ and IFN-γ$^+$ or TNF-α$^+$ over time. (G) Gating strategy for mono- and bi-functional CD4$^+$ T cells. (H) Proportions of mono- and bi-functional CD4$^+$ T cells post-vaccination across groups. Kruskal-Wallis test: *$p \leq 0.05$, **$p \leq 0.01$, ***$p \leq 0.001$, ****$p \leq 0.0001$. (For interpretation of the references to colour in this figure legend, the reader is referred to the web version of this article.)

alpha (TNF-α) production in the CD40L$^+$ population (Fig. 2D). The peak response was observed one month after the second dose. After five months from the second dose, the percentage of CD40L$^+$ cytokine-producing CD4$^+$ T cells decreased and remained stable throughout the analysis (Fig. 2E). Cytokine production was comparable among the participant groups (Fig. 2F). No differences in mono-functional or bi-functional T cells were observed, with the most of cytokine-producing cells being mono-functional (TNF-α$^+$) in all three groups (Fig. 2G and H).

To evaluate the SARS-CoV-2 Spike-specific CD8$^+$ response, we analyzed the percentage of cytokine-producing cells within the CD69-expressing population (Supp. Fig. 3A). As previously shown, the T cell

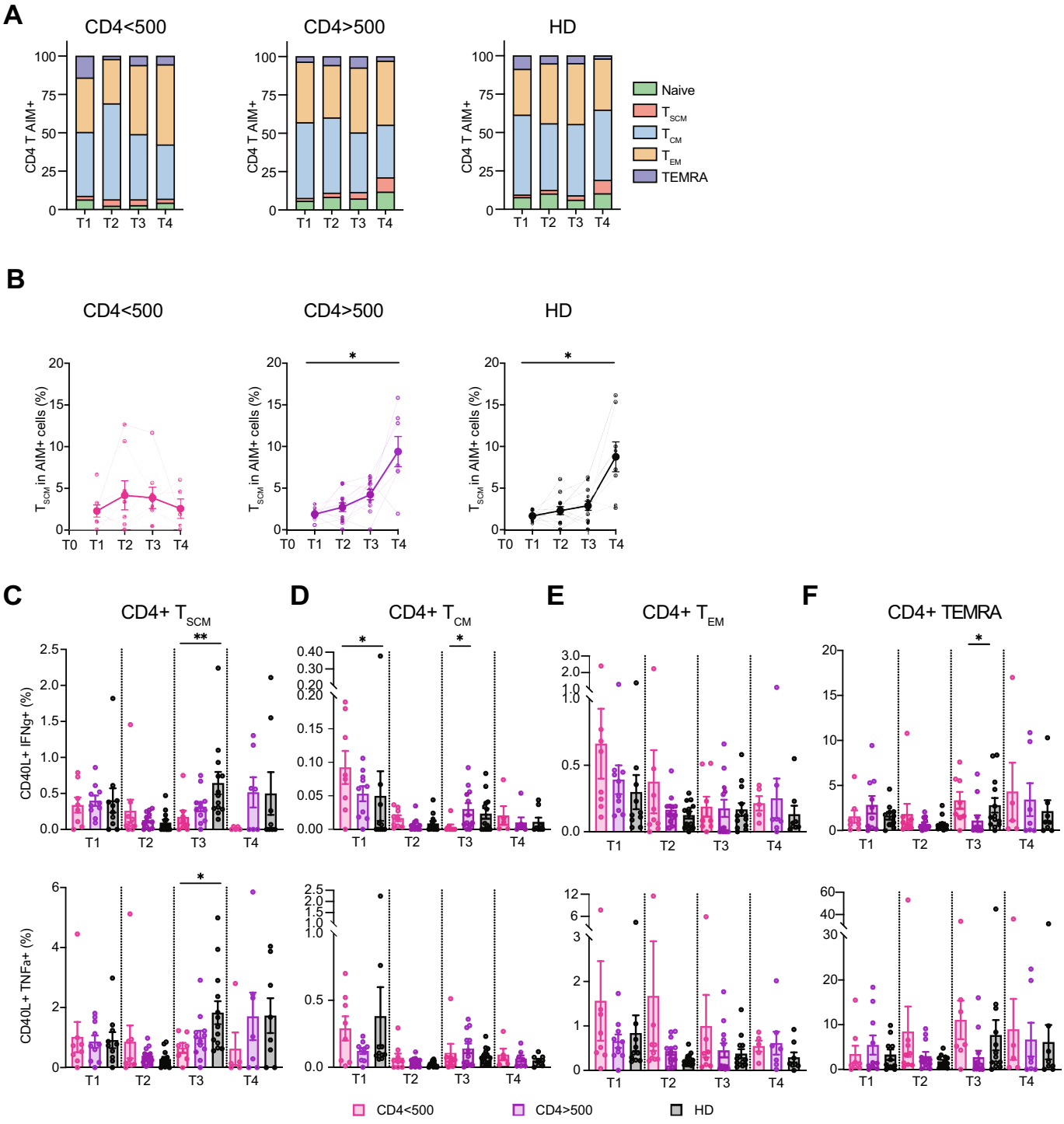

Fig. 3. CD4$^+$ T_{SCM} show a diminished response to SARS-CoV-2 Spike after the third dose booster in PWHIV with an incomplete immune reconstitution. (A) Stacked bar graphs show the subset composition of CD4$^+$ AIM$^+$ T cells in PWHIV with <500 (left panel), >500 CD4$^+$/μL (middle panel) and HDs (right panel), at different time points post vaccination. (B) Longitudinal monitoring of T_{SCM} frequency within AIM$^+$ cells after Spike peptides stimulation in PWHIV with <500 (pink), >500 CD4$^+$/μL (purple), and HDs (black). (Kruskal-Wallis test, *p ≤ 0.05, **p ≤ 0.01, ***p ≤ 0.001, ****p ≤ 0.0001). (C-F) Frequency of CD40L$^+$ IFN-γ$^+$ (upper panels) and CD40L$^+$TNF-α$^+$ (lower panels) following Spike peptides stimulation in the indicated groups across the different memory subsets: T_{SCM} (C), T_{CM} (D), T_{EM} (E) and TEMRA (F). Kruskal-Wallis test (*p ≤ 0.05, **p ≤ 0.01, ***p ≤ 0.001, ****p ≤ 0.0001. (For interpretation of the references to colour in this figure legend, the reader is referred to the web version of this article.)

response was dominated by $CD4^+$ T cells, and the detection of $CD8^+$ specific lymphocytes was more challenging (41). We observed an increasing trend in CD69 + TNF-α^+ and $CD69^+$ IFN-γ^+ $CD8^+$ T cells in all three groups one month after the second dose, which tended to decrease with a minimal boost after the third dose (Supp. Fig. 3B).

No differences were observed in $CD69^+$TNF-α^+ or $CD69^+$IFN-γ^+ cells post-stimulation with the SARS-CoV-2 Spike peptides among the three participant groups, and the percentage of mono-functional or bi-functional $CD8^+$ T cells was similar in the three groups at all time points (Supp. Fig. 3C and D).

In conclusion, our analysis of SARS-CoV-2-specific T cell responses in PWHIV reveals a robust $CD4^+$ T cell response to SARS-CoV-2 Spike across all participants one month after the second vaccine dose (T1). The response gradually waned by the five-months (T2) mark in all the participants and was similarly boosted by the third dose (T3) of the vaccine.

Importantly, PWHIV with a $CD4^+$ T cell count below 500 cells/μL did not show a defect in the total cellular immune response elicited by the vaccine but rather an unexpectedly higher proportion of AIM^+ $CD4^+$ T cells than HDs at multiple time points, suggesting a heightened but potentially transient activation in this subgroup. This increase in AIM^+ $CD4^+$ T cells did not result in differences in cytokine production in response to SARS-CoV-2 Spike peptides re-stimulation.

3.4. $CD4^+$ T_{SCM} show a diminished response to SARS-CoV-2 spike after the third dose booster in PWHIV with an incomplete immune reconstitution

We next examined the contribution of individual $CD4^+$ T memory subsets to the pool of AIM^+ cells. Subsets were defined based on the differential expression of CD45RA, CCR7, and CD95, enabling distinction among Naïve, T_{SCM}, T_{CM}, T_{EM}, and TEMRA cells (Supp. Fig. 4A) [4,41–44].

At baseline (T0), we assessed the percentage of each subset within the $CD4^+$ T cell pool for each participant. As previously reported, PWHIV exhibited a notable reduction in the proportion of Naïve T cells and an expansion of the T_{EM} compartment compared to HDs, with this shift being most pronounced in participants with $CD4^+$ T cell count below 500 cells/μL (Supp. Fig. 4B) [45–47]. The proportions of these subsets remained stable throughout the study duration (Supp. Fig. 4C).

When analyzing the composition of the $CD4^+$ AIM^+ pool, we observed a consistent predominance of the T_{CM} and T_{EM} subsets across all time points in the three groups, as previously reported (Fig. 3A) [2,48]. Notably, the contribution of T_{SCM} to the AIM^+ $CD4^+$ T cell pool increased over time in both HDs and PWHIV with $CD4^+$ T cell count exceeding 500 cells/μL. In contrast, this trend was absent in PWHIV with $CD4^+$ T cell count below 500 cells/μL, where the presence of T_{SCM} within the AIM^+ pool remained unchanged (Fig. 3A, B). No statistically significant differences were observed in the other subsets (Supp. Fig. 4D).

We conducted a longitudinal analysis of the immune response to the SARS-CoV-2 Spike elicited by vaccination in each subset by monitoring the percentage of cells producing IFN-γ and TNF-α among those expressing CD40L at various time points post-vaccination. When comparing IFN-γ and TNF-α production across $CD4^+$ T cell subsets, we found that TEMRA cells consistently produced the highest levels of these cytokines across all three groups, followed by T_{EM} and T_{SCM} subsets, which exhibited comparable cytokine production. T_{CM} cells produced the lowest levels of cytokines upon SARS-CoV-2 Spike peptide re-stimulation (Supp. Fig. 4E).

Across all groups, we observed an increase in SARS-CoV-2 Spike-specific cells in the analyzed subsets after the second vaccine dose (T1). However, CD40L expression and cytokine production declined consistently across all subsets five months following the second dose (T2) (Supp. Fig. 5A-D).

Importantly, the third vaccine dose (T3) significantly increased the percentage of SARS-CoV-2 Spike-specific T_{SCM} cells in HDs and PWHIV with $CD4^+$ T cell count above 500 cells/μL, with levels remaining stable at T4. In contrast, PWHIV with $CD4^+$ T cell count below 500 cells/μL did not exhibit an increase in Spike-specific T_{SCM} following the third dose, indicating a diminished response in this subgroup (Supp. Fig. 5A).

In T_{CM} cells, the third dose modestly boosted responses in PWHIV with $CD4^+$ T cell count above 500 cells/μL, and a similar trend was observed in HDs (Supp. Fig. 5B).

The T_{EM} response declined by five months post-second dose but remained stable in all three groups (Supp. Fig. 5C).

The TEMRA response showed high variability among participants. In HDs, the third dose enhanced the TEMRA response, whereas PWHIV with a $CD4^+$ T cell count of more than 500cells/μL did not exhibit this boost. Interestingly, PWHIV with $CD4^+$ T cell count <500 cells/μL demonstrated an increasing TEMRA response over time, independent of the vaccination boost (Supp. Fig. 5D).

When comparing cytokine production in $CD40L^+$ cells across the groups for each subset, we observed that while the overall Spike-specific response in total $CD4^+$ T cells was similar among the three groups, the percentage of reactive cells within each subset varied significantly. Specifically, T_{SCM} cells isolated from PWHIV with poor immune reconstitution exhibited lower reactivity compared to HDs at later time points (T3 and T4) (Fig. 3C).

In the T_{CM} subset, IFN-γ production was notably higher in PWHIV with $CD4^+$ T cell count <500 cells/μL compared to HDs one month after the second dose. However, by five months, all groups showed a decline in SARS-CoV-2 Spike-specific T_{CM} responses. Only HDs and PWHIV with $CD4^+$ T cell count >500 cells/μL showed a boost in IFN-γ expression following the third dose (Fig. 3D).

For T_{EM} cells, cytokine production tended to be higher in PWHIV with $CD4^+$ T cell count <500 cells/μL at T1 and T2, although this difference did not reach statistical significance. At T3 and T4, cytokine levels in T_{EM} cells were similar across the three groups (Fig. 3E). The response in TEMRA cells was highly heterogeneous. TEMRA cells from PWHIV with $CD4^+$ T cell count <500 cells/μL showed a tendency towards higher cytokine production compared to HDs and PWHIV with $CD4^+$ T cell count >500 cells/μL, although variability was substantial (Fig. 3F).

We next examined the $CD8^+$ T cell subsets responses elicited by the SARS-CoV-2 vaccine. $CD8^+$ T memory cells were categorized into T_{SCM}, T_{CM}, T_{EM}, and TEMRA subsets, based on the expression of CD45RO, CCR7, and CD95 (Supp. Fig. 6A).

Notably, the percentage of $CD8_+$ T cells was higher in PWHIV compared to HDs, especially in PWHIV with $CD4^+$ T cell count <500 cells/μL reflecting the depletion of $CD4^+$ T cells (Supp. Fig. 6B). This proportion remained stable throughout the study (Supp. Fig. 6C). We observed a depletion of Naïve $CD8^+$ T cells in PWHIV, particularly in those with $CD4^+$ T cell count below 500 cells/μL, consistent with previous reports (Supp. Fig. 6D) [40,49]. With few fluctuations, the distribution of the various subsets within the $CD8^+$ T cell pool remained stable over the course of the study, except a peak in the $CD8^+$ T_{EM} subset in PWHIV with low $CD4^+$ T cell count at T1 (Supp. Fig. 6E).

The overall percentages of $CD69^+$ IFN-γ^+ and $CD69^+$ TNF-α^+ cells within each subset were very low, aligning with our earlier observations for the total $CD8^+$ T cell population. Furthermore, when comparing the percentages of IFN-γ^+ $CD69^+$ and TNF-α^+ $CD69^+$ cells across the different subsets within each group, we observed no substantial differences, unlike the distinct patterns seen in $CD4^+$ T cell subsets (Supp. Fig. 6F).

We then longitudinally assessed the percentages of SARS-CoV-2 Spike-specific cells within each $CD8^+$ T cell subset (Supplementary Fig. 7A–D). Detection of Spike-specific responses in $CD8^+$ T cells posed challenges due to individual variability and suboptimal stimulation of this population, as previously reported [40]. A statistically significant increase in the percentage of Spike-specific cells was observed exclusively in the T_{CM} subset. Specifically, we detected an increase in SARS-CoV-2 Spike-reactive T_{CM} cells at T1 in PWHIV with an optimal immune reconstitution and in HDs, which consistently declined over time (Supplementary Fig. 7B). No significant differences were identified

among the three groups (Supplementary Fig. 7E–H).

In summary, our data suggest that while the total $CD4^+$ T cell response towards SARS-CoV-2 Spike peptides was similar in the three groups, specific differences were observed at the level of $CD4^+$ T cell subsets. Notably, we observed a statistically significant impairment in the response of T_{SCM} and T_{CM} in PWHIV with an incomplete immune reconstitution and a tendency for the more differentiated subsets (T_{EM} and TEMRA) to produce higher levels of cytokines. These findings

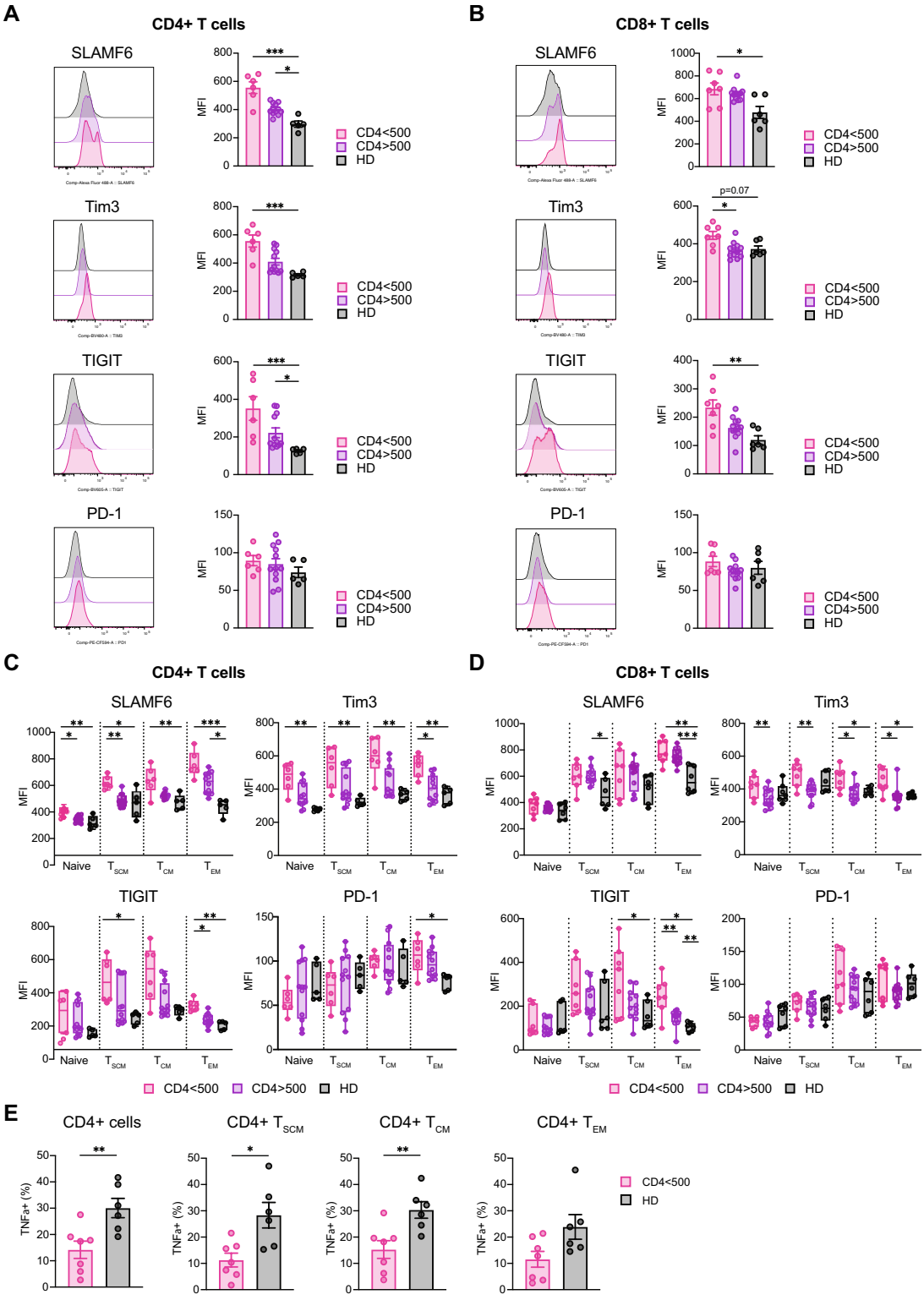

Fig. 4. Expression of Immune Checkpoint Markers is increased in $CD4^+$ T Cell Subsets of PWHIV with an incomplete immune reconstitution.
(A-B) Expression levels of SLAMF6, TIM3, TIGIT and PD-1 were analyzed in total $CD4^+$ (A) and total $CD8^+$ (B) T lymphocytes. Kruskal-Wallis test (*p ≤ 0.05, **p ≤ 0.01, ***p ≤ 0.001, ****p ≤ 0.0001). (C-D) Comparison of immune checkpoint markers expression among the indicated groups in the different $CD4^+$ (C) and $CD8^+$ (D) T cell subsets. Kruskal-Wallis test (*p ≤ 0.05, **p ≤ 0.01, ***p ≤ 0.001, ****p ≤ 0.0001). (E) Percentage of TNFα producing cells within total $CD4^+$ T cells and $CD4^+$ T cell subsets following CD3/CD28 stimulation. (Mann-Whitney statistical test, *p ≤ 0.05, **p ≤ 0.01, ***p ≤ 0.001, ****p ≤ 0.0001).

suggest that the immune dysregulation that characterizes PWHIV, who do not restore a normal immune system despite ART, may influence the vaccine response in specific subsets.

3.5. Expression of immune checkpoint markers is increased in CD4$^+$ T cell subsets of PWHIV with an incomplete immune reconstitution

Persistent inflammation in chronic infections, such as HIV, significantly affects immune homeostasis and T-cell function. In PWHIV, T cells exhibit increased expression of immune checkpoint markers and T-cell activation, which are associated with suboptimal immune reconstitution, despite undetectable viremia [50–52].

To investigate the potential differences in the expression of immune checkpoint markers within our cohort, we analyzed, at T0, the expression of T-cell immunoglobulin and mucin-domain containing-3 (TIM-3), programmed cell death protein 1 (PD-1) and T-cell immunoreceptor with Ig and ITIM domains (TIGIT) as well as the Self-ligand receptor of the signaling lymphocytic activation molecule family member 6 (SLAMF6) in total CD4$^+$ and CD8$^+$ T cells isolated from PWHIV<500 CD4$^+$ T cells/μL, PWHIV>500 CD4$^+$ T cells/μL and HDs.

In PWHIV with incomplete immune reconstitution, total CD4$^+$ T lymphocytes exhibited consistently higher expression of SLAMF6, TIM-3, and TIGIT compared to HDs. Among individuals with CD4$^+$ T cell count below 500 cells/μL, SLAMF6 and TIGIT expression was significantly elevated relative to HDs. No significant differences across the three groups were observed in PD-1 expression (Fig. 4A). Similarly, higher expression of SLAMF6, TIM-3, and TIGIT was observed in CD8$^+$ T lymphocytes from PWHIV with CD4$^+$ T cell count below 500 cells/μL compared to HDs (Fig. 4B).

Since we observed a functional impairment in specific CD4$^+$ T cell subsets of PWHIV with low CD4$^+$ T cell count, we next assessed the expression of immune checkpoint markers across the different subsets of CD4$^+$ T cells within the cohort. Consistent with expectations, less differentiated T cell subsets, such as Naïve and T_{SCM} cells, exhibited lower expression levels of SLAMF6, TIM-3, TIGIT, and PD-1 compared to more differentiated subsets across all three groups (Supp. Fig. 8A). When comparing immune checkpoint marker expression among groups, individuals with CD4$^+$ T cell count below 500 cells/μL consistently demonstrated higher expression of SLAMF6 and TIM-3 across all subsets relative to both HDs and individuals with CD4$^+$ T cell count exceeding 500 cells/μL. TIGIT expression was elevated in T_{SCM}, T_{CM} and T_{EM} from PWHIV with an incomplete immune reconstitution compared to HD, while differences in PD-1 expression were observed exclusively in the effector memory subset (Fig. 4C).

Analysis of immune checkpoint marker expression across CD8$^+$ T cell subsets showed again a consistent trend where SLAMF6, TIGIT, and PD-1 expression was lower in the less differentiated CD8$^+$ T cell subsets (Supp. Fig. 8B).

In PWHIV with incomplete immune reconstitution, CD8$^+$ T_{SCM} and T_{EM} showed higher levels of SLAMF6, while all subsets from PWHIV with a CD4$^+$ T cell count <500 had higher expression of TIM-3 compared to HDs. Increased TIGIT expression in individuals with an incomplete immune reconstitution was limited to the T_{CM} and T_{EM} subsets. As with CD4$^+$ T cells, no differences in PD-1 expression were detected across CD8$^+$ T cell subsets (Fig. 4D).

Given the elevated levels of immune checkpoint markers observed in CD4$^+$ T cells from PWHIV with incomplete immune reconstitution compared to HDs, we investigated whether this correlated with a diminished capacity to respond to stimulation.

To assess this, we stimulated CD4$^+$ T cells with a CD3/CD28 agonist and found that total CD4$^+$ T cells, as well as individual subsets, including T_{SCM}, T_{CM}, and T_{EM}, from PWHIV with CD4$^+$ T cell count below 500 cells/μL exhibited reduced TNF-α production in response to stimulation compared to HDs (Fig. 4E and Supp. Fig. 8C).

In summary, CD4$^+$ T cells from PWHIV with incomplete immune reconstitution exhibit both elevated immune checkpoint markers expression and a reduced capacity to produce TNF-α upon stimulation. These findings suggest that immune exhaustion may contribute to impaired T cell functionality in this subgroup, potentially impacting their overall immune response.

3.6. PWHIV with incomplete immune reconstitution exhibit an elevated percentage of T_{CM} and T_{SCM} co-expressing PD-1 and TIGIT

Recent findings have refined our understanding of T cell dysfunction by identifying distinct subsets T_{SCM} and T_{CM} with divergent functional potentials. Specifically, a subpopulation of CD8$^+$ T_{SCM} and T_{CM} cells expressing the inhibitory receptors PD-1 and TIGIT has been characterized as committed to an exhausted-like lineage. These cells defined as T progenitor exhausted-like (T_{PEX}) display diminished proliferative capacity and cytokine production. In contrast, T_{SCM} and T_{CM} progenitors lacking these inhibitory markers exhibit classical stem-like features, including robust proliferation and responsiveness to stimulation. This distinction highlights the heterogeneity within memory T cell compartments and suggests that inhibitory receptor expression serves as a defining marker of lineage commitment and functional capacity [32].

Considering that chronic infections are associated with general T cell exhaustion and preferentially generate antigen-specific T_{PEX} cells, we first investigated whether CD8$^+$ T_{PEX} were present at different frequencies across our cohorts [32,53].

Analysis of the expression of PD-1 and TIGIT within CD8$^+$ T_{SCM} and T_{CM} subsets in our cohort revealed that PWHIV with incomplete immune reconstitution displayed a significantly higher percentage of CD8$^+$ T_{SCM} and T_{CM} co-expressing PD-1 and TIGIT compared to HDs and PWHIV with optimal immune reconstitution (Fig. 5A, B).

Of note, we compared the expression of SLAMF6 (Fig. 5C, D) and CD38 (Fig. 5E, F) in CD8$^+$ T_{CM} PD-1$^+$TIGIT$^+$ and T_{CM} PD-1$^-$TIGIT$^-$ as well as in T_{SCM} PD-1$^+$TIGIT$^+$ and T_{SCM} PD$^-$1-TIGIT$^-$, and we observed that the expression of these two markers was higher in the population co-expressing PD-1 and TIGIT, suggesting an exhausted/activated phenotype of these populations [54–56].

We next evaluated whether similar PD-1$^+$TIGIT$^+$ cells could be identified within CD4$^+$ T_{SCM} and T_{CM} compartments. As observed in CD8$^+$ T cells, subsets of CD4$^+$ T_{SCM} and T_{CM} also co-expressed these inhibitory markers (Fig. 5G, Supp. 8D). When comparing PD-1$^+$TIGIT$^+$ frequencies across participant groups, we found that individuals with CD4$^+$ T cell count below 500 cells/μL exhibited markedly higher percentages of these exhausted-like progenitors in both CD4$^+$ T_{SCM} and T_{CM} subsets compared to those with CD4$^+$ T cell count above 500 cells/μL and HDs (Fig. 5H). Notably, in PWHIV, the frequency of PD-1$^+$TIGIT$^+$ CD4$^+$ T_{SCM} inversely correlates with CD40L upregulation and TNF-α and IFNγ production by T_{SCM} upon restimulation with SARS-CoV-2 Spike peptides (Supp. 8E). As already noted for CD8$^+$ T cells, also in CD4$^+$ T_{CM} PD-1$^+$TIGIT$^+$ and CD4 T_{SCM} PD-1$^+$TIGIT$^+$ expressed higher levels of SLAMF6 and CD38 compared to the corresponding PD$^-$1-TIGIT$^-$ populations (Fig.5I-L).

These findings suggest that an exhausted-like progenitor population is present not only in CD8$^+$ T but also in CD4$^+$ T lymphocytes and the percentage of these cells is enriched in PWHIV with suboptimal immune reconstitution compared to HDs, potentially contributing to their impaired immune recovery.

3.7. GSK3β inhibition restores TCF-1 expression in CD4$^+$ T_{SCM} cells from PWHIV with incomplete immune reconstitution

The Wnt/β-catenin and mTOR pathways are pivotal regulators of the stemness properties of T_{SCM} [57–61]. Disruptions in the Wnt/β-catenin pathway, particularly due to aging and inflammation, have been shown to impair the proliferative capacity and functionality of T_{SCM}. Specifically, T_{SCM} isolated from older donors exhibit diminished T cell factor-1 (TCF-1) expression and decoupling from SLAMF6 expression. This decoupling correlates with reduced functionality, underscoring the

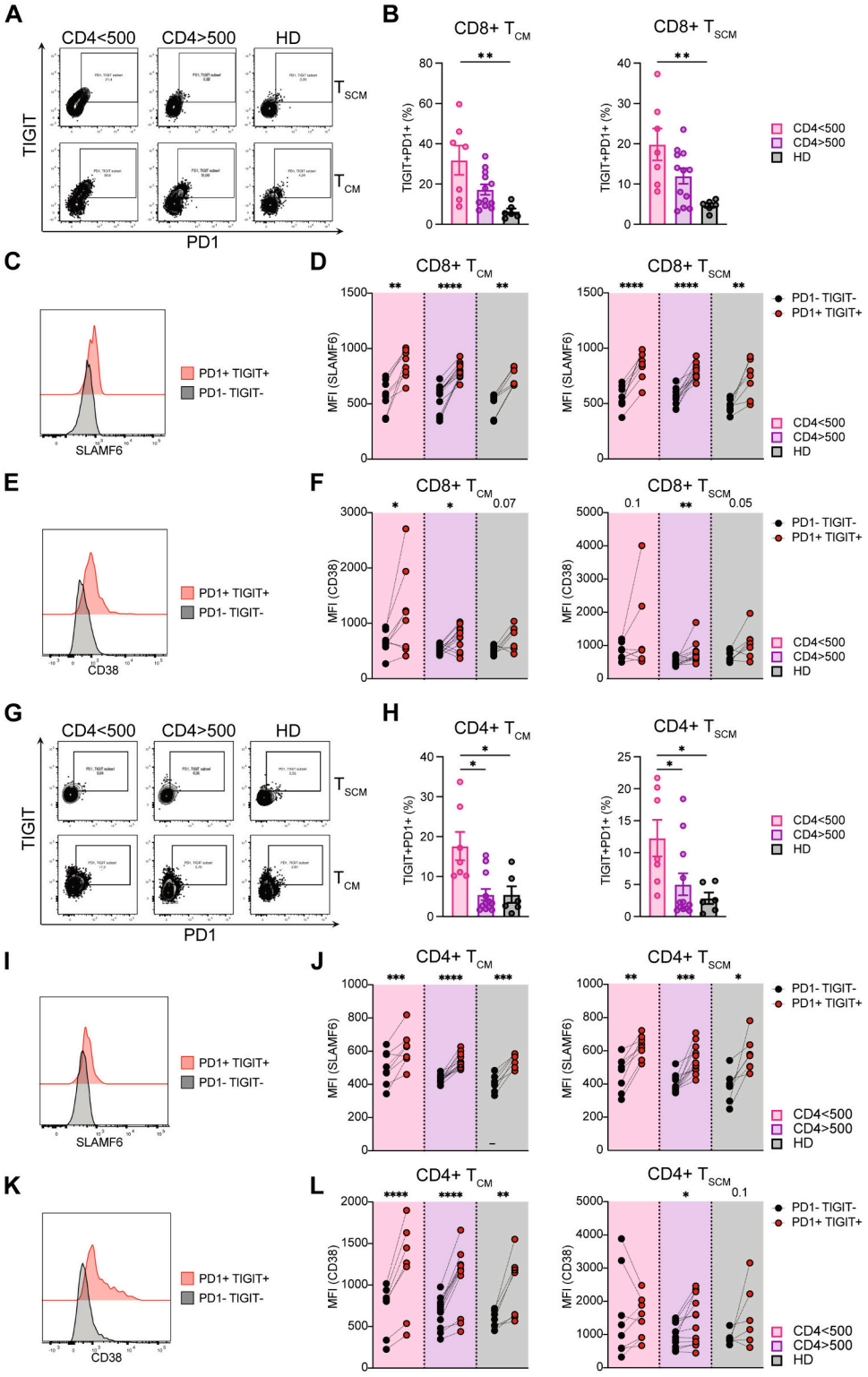

Fig. 5. PWHIV with incomplete immune reconstitution exhibit an elevated percentage of T_{CM} and T_{SCM} co-expressing PD-1 and TIGIT.
(A) Representative flow cytometry plot for the identification of PD-1 and TIGIT expressing cells in $CD8^+$ T_{CM} and T_{SCM}. (B) The percentage of PD-1^+ $TIGIT^+$ cells in $CD8^+$ T_{CM} and T_{SCM} was compared across the groups of participants. Kruskal-Wallis test. (C-D) Representative histogram (C) and quantification (D) of SLAMF6 expression in PD-1^+ $TIGIT^+$ and PD-1^- $TIGIT^-$ in $CD8^+$ T_{CM} and T_{SCM}. Ratio paired *t*-test (*p ≤ 0.05, **p ≤ 0.01, ***p ≤ 0.001, ****p ≤ 0.0001). (*E*-F) Representative histogram (E) and quantification (F) of CD38 expression in the indicated populations. (G) Representative flow cytometry plot showing PD-1 and TIGIT expression in $CD4^+$ T_{CM} and T_{SCM}. (H) Comparison of the percentage of PD-1^+ $TIGIT^+$ cells in $CD4^+$ T_{CM} and T_{SCM} across participant groups. Kruskal-Wallis test (*p ≤ 0.05, **p ≤ 0.01, ***p ≤ 0.001, ****p ≤ 0.0001). (I-J) Representative histogram (I) and quantification (J) of SLAMF6 expression in PD-1^- $TIGIT^-$ and PD-1^+ $TIGIT^+$ in $CD4^+$ T_{CM} and T_{SCM}. Ratio paired t-test (*p ≤ 0.05, **p ≤ 0.01, ***p ≤ 0.001, ****p ≤ 0.0001). (K-L) Representative histogram (K) and quantification (L) of CD38 expression in PD-1^- $TIGIT^-$ and PD-1^+ $TIGIT^+$ $CD4^+$ T cells. Ratio paired t-test (*p ≤ 0.05, **p ≤ 0.01, ***p ≤ 0.001, ****p ≤ 0.0001).

importance of the TCF-1–SLAMF6 axis in maintaining T_{SCM} integrity [60,62].

To investigate this further, we analyzed $CD4^+$ T cells from PWHIV with incomplete immune reconstitution, specifically comparing TCF-1 and SLAMF6 expression levels to those in HDs. In individuals with a $CD4^+$ T cell count below 500 cells/μL, we observed consistently reduced TCF-1 expression and elevated SLAMF6 expression across all $CD4^+$ T cell subsets, suggesting a disruption in the molecular pathways regulating T cell stemness and homeostasis (Fig. 6A–B and Fig.4C). As expected, naïve, T_{SCM}, and T_{CM} subsets showed the highest TCF-1 expression, while T_{EM} cells exhibited the lowest (Supp. Fig. 8F and G). In contrast, SLAMF6 expression increased progressively with differentiation (Supp. Fig. 8A).

Notably, similar alterations in the balance between TCF-1 and SLAMF6 have been reported in T_{SCM} cells from young versus aged donors, supporting the hypothesis that these changes reflect dysregulation of the Wnt-dependent signaling network critical for maintaining T_{SCM} homeostasis [60,63].

The inhibition of glycogen synthase kinase-3β (GSK3β), a critical regulator of the Wnt/β-catenin pathway, restored the stemness of $CD4^+$ T_{SCM} from older individuals and enhanced the responses of $CD8^+$ T cells from HIV-positive individuals [59,60]. Thus, we investigated whether GSK3β inhibition could restore the impaired stemness and function of $CD4^+$ T_{SCM} in PWHIV with incomplete immune reconstitution within our cohort.

First, we assessed the effect of GSK3β inhibition on TCF-1 and SLAMF6 expression levels in $CD4^+$ T cells. PBMCs isolated from PWHIV and HDs were treated with the GSK3β inhibitor TWS119. The treatment significantly reduced GSK3β activity, as indicated by decreased phosphorylated S6 (pS6) levels following anti-CD3/CD8 stimulation (Supp. Fig. 9A and B) [59].

Interestingly, treatment with TWS119 resulted in a trend of increased TCF-1 expression only in $CD4^+$ T cells isolated from PWHIV with incomplete immune reconstitution, which reached statistical significance in the T_{SCM} subset (Fig. 6C, D and Supp. Fig. 9C). A trend towards a reduction of SLAMF6 expression was also observed after treatment with TWS119 (Supp. Fig. 9D and E).

We then asked whether GSK3β inhibition could reduce the percentage of $PD\text{-}1^+TIGIT^+$ cells within T_{SCM} and T_{CM}. After TWS119 treatment, the rate of $PD\text{-}1^+TIGIT^+$ populations remained unaltered (Supp. Fig. 9F). Nevertheless, overall expression of TIGIT in T_{SCM} and T_{CM} was decreased after TWS119 treatment in both PWHIV and HDs (Fig. 6E and F). A similar trend of diminished TCF-1 expression was also observed in $CD8^+$ T cell subsets from PWHIV, which was slightly increased, but not fully restored by GSK3β inhibition (Supp. Fig. 9G and H).

These results suggest that targeting GSK3β activity can effectively rebalance the TCF-1–SLAMF6 axis in cases where it is disrupted, such as in prolonged inflammation caused by chronic infections.

To determine if this phenotype was associated with a more functional state of T_{SCM} in PWHIV, we stimulated TWS119-treated PBMCs from participants with various stimuli. We first analyzed the effect of TWS119 on T cell response following CD3/CD28 stimulation. TWS119 dramatically reduced the TNF-α production in total $CD4^+$ and $CD8^+$ T cells (Supp. Fig. 10A, 10B); thus, we did not investigate further the cytokine production upon CD3/CD28 stimulation within T cell subsets. When cells were stimulated with the bacterial toxin SEB, we also observed a decrease in TNF-α production by total $CD4^+$ T cells (Supp. Fig. 10A). However, this decrease was not as dramatic as that observed with CD3/CD28 stimulation. In total $CD8^+$ T cells, TWS119 treatment had a variable effect on cytokine production following SEB stimulation and the trend was unclear (Supp. Fig. 10B). We then investigated the effects of TWS119 on SEB-induced cytokine production within T memory subsets (Supp. Fig. 10C and D). Among the $CD4^+$ T memory subsets, we observed an overall decrease in TNF-α production, which was more striking in the more differentiated subsets, especially in HDs (Supp. Fig. 10C). In $CD8^+$ T memory subsets, we observed a decreased TNF-α production in T_{SCM}, which reached statistical significance only in HDs, and a more variable effect with no significant differences among the other subsets (Supp. Fig. 10D).

Finally, we examined the effect of TWS119 on the T cell response to SARS-CoV-2 Spike peptides. In this case, an increase in TNF-α production was observed in $CD4^+$ T_{SCM} in all the groups which, however, did not reach statistical significance (Fig. 6G and H). A similar trend of increased TNF-α production was observed in $CD8^+$ T_{SCM} (Supp. Fig. 10F), which reached statistical significance only among HDs.

In total $CD4^+$ and $CD8^+$ T cells and the other memory subsets the effect was more variable. TWS119 decreased the response to SARS-CoV-2 Spike peptide only in total $CD4^+$ T and T_{CM} from HD (Supp. Fig. 10E), while an increase in the response of $CD8^+$ T_{SCM} from HD was observed (Supp. Fig. 10F).

These findings underscore the potential of GSK3β inhibitors as a promising therapeutic tool for restoring T cell stemness in PWHIV with an incomplete immune reconstitution.

Nevertheless, the variable effect of TWS119 in different subsets of T cells and in different stimulation contexts should be considered. Indeed, TWS119 appears to act mainly as an immune-suppressor in the case of TCR co-stimulation and SEB stimulation; however, it may specifically enhance T_{SCM} response to recall viral antigens, such as SARS-CoV-2 Spike peptides.

4. Discussion

T_{SCM} play a crucial role in sustaining long-term immune memory, a feature particularly valuable in the context of vaccination, where durable protection is essential [1–5].

This is especially relevant for vulnerable populations such as PWHIV, whose compromised immune system may affect their ability to mount and maintain effective vaccine-induced immune responses. Indeed, defects in vaccine-induced immune responses have been reported in this population [8–13]. We took advantage of the SARS-CoV-2 vaccination campaign to longitudinally investigate the dynamics of T_{SCM} responses to Spike peptides in this population, with a specific focus on individuals with an incomplete immune reconstitution despite controlled viremia.

In general, studies evaluating the response to COVID-19 vaccines in PWHIV suggest that SARS-CoV-2 vaccination is generally safe and effective in this population. Several studies have demonstrated that PWHIV can generate a robust antibody response following vaccination, although the magnitude and durability of the response may vary compared to individuals without HIV [35,64,65].

The quality of the immune response to COVID-19 vaccines in PWHIV is influenced by several factors. These include the individuals' level of immune suppression, $CD4^+$ T cell count, viral load, and use of antiretroviral therapy (ART). Individuals with well-controlled HIV, higher $CD4^+$ T cell count, and undetectable viral loads tend to mount both a cellular and a robust humoral immune response. However, individuals with a low $CD4^+$ T cell count and low CD4/CD8 ratio show an impaired and less durable response [16,19,20].

To understand the impact of immune reconstitution on the T_{SCM} response, we stratified the PWHIV cohort into two groups based on their $CD4^+$ T cell count (<500 cells/μL and $>$ 500 cells/μL). Of note, the group characterized by lower $CD4^+$ T cell count also exhibited lower CD4/CD8 ratio (median 0.35) and higher occurrence of previously experienced AIDS (7/9), compared to the other group (1.1 median CD4/CD8 ratio, 0/13 AIDS).

First of all, we characterized the humoral response and we observed that following the administration of two doses of the mRNA vaccine, PWHIV exhibited a slightly impaired neutralization capacity towards the B.1.617.2 variant compared to healthy individuals. Neutralization capacity decreased after five months, regardless of $CD4^+$ T cell count. The decrease in neutralizing activity towards the WT Spike was significantly higher in PWHIV compared to HDs. However, after the administration of the third dose, significant differences between PWHIV and

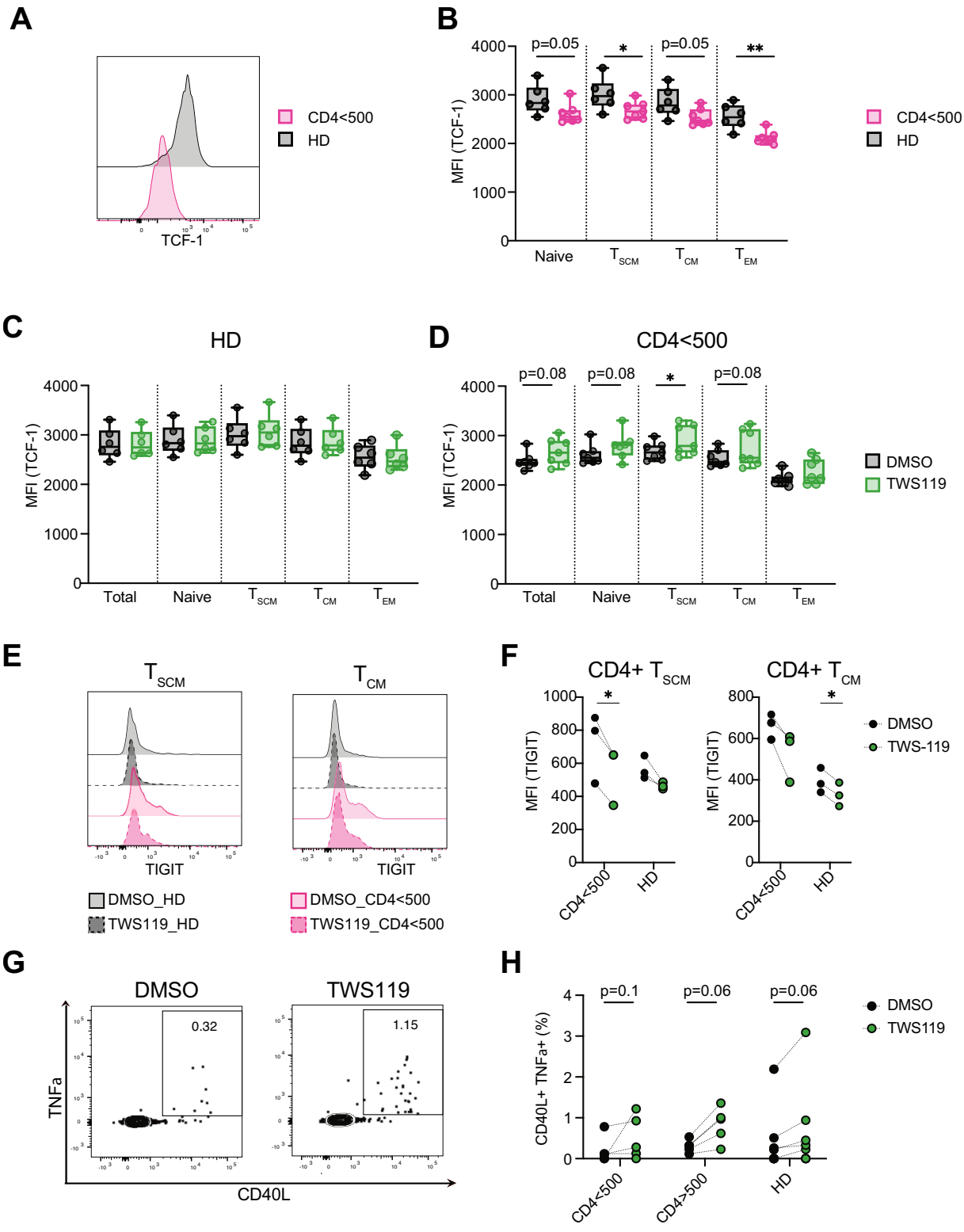

Fig. 6. GSK3β inhibition restores TCF-1 expression in CD4$^+$ T_{SCM} cells from PWHIV with incomplete immune reconstitution.
(A-B) Representative histogram plot (A) and quantification (B) of TCF-1 expression in CD4$^+$ T cells subsets in HD and PWHIV with <500 CD4$^+$/μL. (Mann-Whitney test *p ≤ 0.05, **p ≤ 0.01, ***p ≤ 0.001, ****p ≤ 0.0001). (C-D) Effect of TWS119 treatment on TCF-1 expression in total CD4$^+$ T lymphocytes and CD4$^+$ T cell subsets in HD (C) and PWHIV with <500 CD4$^+$/μL (D). The graphs show differences between untreated controls (black) and TWS119 treated samples (green). (Wilcoxon signed-rank test *p ≤ 0.05, **p ≤ 0.01, ***p ≤ 0.001, ****p ≤ 0.0001). (E) Representative histogram of TIGIT expression in CD4$^+$ T_{SCM} and T_{CM} following TWS119 treatment. (F) Quantification of TIGIT expression with and without TWS119 treatment in CD4$^+$ T_{SCM} and T_{CM} (Ratio paired t-test *p ≤ 0.05, **p ≤ 0.01, ***p ≤ 0.001, ****p ≤ 0.0001). (G) Representative flow cytometry plot showing the TNF-α production in CD40L$^+$ CD4$^+$ T_{SCM} after SARS-CoV-2 Spike peptides stimulation. (H) Quantification of TNF-α production in CD40L$^+$ CD4$^+$ T_{SCM} after SARS-CoV-2 Spike peptides stimulation, with and without TWS119 treatment. (Wilcoxon test *p ≤ 0.05, **p ≤ 0.01, ***p ≤ 0.001, ****p ≤ 0.0001). (For interpretation of the references to colour in this figure legend, the reader is referred to the web version of this article.)

healthy donors were no longer observed, highlighting the importance of the booster in enhancing the immune response, especially in PWHIV, as noted earlier [66].

When characterizing the total $CD4^+$ T cell response targeting the SARS-CoV-2 Spike protein, we did not observe significant differences between the two groups of PWHIV and HDs. Notably, individuals with a low $CD4^+$ T cell count displayed increased production of TNF-α, consistent with previous reports [67]. However, when examining the response of specific T cell subsets, we observed that only in HDs and PWHIV with $CD4^+$ T cell count exceeding 500 cells/μl, the contribution of T_{SCM} to the AIM^+ $CD4^+$ T cell pool increased over time while in PWHIV with $CD4^+$ T cell count below 500 cells/μL the percentage of T_{SCM} within the AIM^+ pool remained unchanged.

In addition, we observed that the $CD4^+$ T_{SCM} response to SARS-CoV-2 Spike on these participants was impaired one month and six months after the booster dose, indicating a potential defect in T_{SCM} function. Importantly, comparable responses at earlier time points suggest that there is no defect in memory formation but rather a deficiency in cytokine production upon restimulation.

The analysis of T_{SCM} cells provides critical insights into the longevity and quality of the immune response in PWHIV. An impairment of T_{SCM} response could have significant implications for the durability of the vaccine-induced immune response in this population [3,5,68,69]. The diminished response of T_{SCM} cells in PWHIV with low $CD4^+$ T cell count was accompanied by an increased expression of immune checkpoint markers such as SLAMF6, TIM-3, and TIGIT. These markers are associated with T cell exhaustion, which is a hallmark of chronic HIV infection [7,26,70,71].

Recently, distinct subsets of stem-like $CD8^+$ T cells committed to an exhausted-like lineage ($CD8^+$ T_{PEX}) have been characterized. These cells express the inhibitory receptors PD-1 and TIGIT and exhibit reduced proliferative capacity and cytokine production compared to their $PD\text{-}1^-TIGIT^-$ counterparts [32]. In our study, we observe for the first time a marked enrichment of $CD8^+$ T_{PEX} cells in PWHIV, particularly those with low $CD4^+$ T cell count, highlighting a potential link between immune exhaustion and impaired immune recovery.

Importantly, we also identify, for the first time, a population of $CD4^+$ T_{SCM} and $CD4^+$ T_{CM} cells co-expressing PD-1 and TIGIT, phenotypically resembling the $CD8^+$ T_{PEX} subset. The $PD\text{-}1^+TIGIT^+$ $CD4^+$ T_{SCM} and T_{CM} cells show elevated expression of SLAMF6 and CD38, markers associated with activation and differentiation, suggesting that a similar exhausted precursor population may exist within the $CD4^+$ compartment.

Taking together these data suggest that the elevated expression of checkpoint markers in less differentiated T cell subsets and the increases percentage of T_{PEX} in both $CD4^+$ and $CD8^+$ T cell compartments, could be limiting the efficacy of vaccination in these individuals.

Therapeutic strategies to improve T cell function in PWHIV may include immune checkpoint inhibitors and agents targeting differentiation and metabolic pathways, such as Wnt/β-catenin and mTOR pathways. GSK3β inhibition, for instance, has been shown to enhance $CD8^+$ T cell function in PWHIV and restore T_{SCM} stemness in aged individuals [59,60]. In our study, treatment with the GSK3β inhibitor TWS119 restored TCF-1 expression and reduced TIGIT levels in $CD4^+$ T_{SCM} and T_{CM} from PWHIV with low $CD4^+$ count. However, it also impaired cytokine production, particularly following CD3/CD28 stimulation, and to a lesser extent after SEB exposure, especially in more differentiated subsets. On the other hand, antigen-specific stimulation with SARS-CoV-2 peptides led to a modest increase in TNF-α, limited to $CD4^+$ T_{SCM}. These variable effects likely stem from the distinct signaling pathways engaged by the different stimuli utilized. Indeed, CD3/CD28 co-stimulation strongly activates the PI3K/Akt/mTOR axis, driving proliferation and effector function [72,73], while SEB also relies on other pathways [74–76]. Antigen-specific stimulation is more variable, depending on TCR affinity and cytokine context. It has been reported that rapamycin boosts T cell responses during infection but not transplantation suggesting that mTOR inhibition may differentially affect immune responses, for example by suppressing polyclonal activation while preserving or enhancing antigen-specific memory [77].

T cells' differentiation state further influences mTOR dependency—naïve and T_{SCM} rely on oxidative metabolism and are more resistant to mTOR inhibition, while glycolysis-dependent effector cells are more vulnerable [58,72,78]. This may explain why GSK3β inhibition preserved stem-like traits but suppressed effector functions.

We are aware that our study has several limitations. The small sample size ($n = 22$ PWHIV, $n = 14$ HDs) and the male predominance in the PWHIV group could limit generalizability. The presence of unreported SARS-CoV-2 infections in some participants could have influenced immune responses. Additionally, our specific focus on the mRNA-1273 vaccine means that the findings may not be applicable to other vaccines. While we conducted a thorough characterization of the various $CD4^+$ T cell memory subsets, we did not investigate T follicular helper (Tfh) cells, whose low numbers in PWHIV have been implicated in poor humoral responses to vaccination [79]. We have a limited evaluation of clinical outcomes and faced challenges in detecting robust $CD8^+$ T cell responses. However, our study provides novel insights into the nuanced immune responses of PWHIV to SARS-CoV-2 vaccination, particularly highlighting potential vulnerabilities in those with lower $CD4^+$ T cell count.

The impaired response in T_{SCM} cells, the heightened expression of exhaustion markers and the increased percentage of T_{PEX} in PWHIV with low $CD4^+$ T cell count highlight the need for additional interventions to optimize vaccine efficacy in this vulnerable population.

The GSK3β inhibitors could be a promising therapeutic tool to improve T cell stemness and functions [80,81]. However, its variable effects on different T cell subsets and its immune-suppressive activity upon stronger TCR stimulation have to be considered and further investigated before a clear picture can be drawn [72,78].

Further research into targeted therapies that can enhance T_{SCM} responses and mitigate immune exhaustion will be essential for improving long-term immunity and protection following vaccination in PWHIV.

5. Conclusions

In conclusion, this study demonstrates that while SARS-CoV-2 mRNA vaccination elicits generally robust humoral and cellular immune responses in PWHIV, individuals with incomplete immune reconstitution, marked by low $CD4^+$ T cell counts and low CD4/CD8 ratio, exhibit impaired T_{SCM} responses and increased expression of checkpoint markers such as TIGIT, Tim3, and SLAMF6. In addition, the enrichment of exhausted-like T cell subsets (T_{PEX}) in both $CD4^+$ and $CD8^+$ compartments suggests that immune exhaustion may limit the persistence and quality of vaccine-induced immunity in this population.

Notably, GSK3β inhibition partially restored TCF-1 expression in T_{SCM} and their response towards SARS-CoV2 Spike peptides. Together, these findings reveal critical vulnerabilities in vaccine-induced memory formation in PWHIV with low $CD4^+$ counts and highlight the need for tailored immunotherapeutic strategies to enhance T cell fitness, sustain immune memory, and improve vaccine efficacy in this vulnerable group.

Authors contribution

SS, AL and LM designed the study. SS performed the neutralization assays with the help of GMB, MC, MC and LD. MO performed anti-S and anti-N quantification. SS and GMB performed the flow cytometry experiments, with assistance from MC. AL, GB, SL, AM and AB enrolled the participants. SS, GMB, MC, LD, MC, ND and ES processed the samples. RG, SA, AG and AB designed the clinical study. LM, AL and RDF provided financial support. The manuscript was written by SS, AL and LM.

Acknowledgments

We sincerely thank all study participants. LM was supported by the

Italian Ministry of Health Grant Ricerca Finalizzata GR 2018-12365699 and by Italian Ministry for University and Research Grant PRIN 2022-2022RYNKB5. AL, RDF and RD were supported by EU funding and Italian Ministry for University and Research within the NextGenerationEU-MUR PNRR Extended Partnership initiative on Emerging Infectious Diseases PE00000007 (INF-ACT). RDF is also supported Italian Ministry for University and Research Grants P2022Z8HNC (ENTI-B) and 20224NMLXK. We thank members of the FACS core facility of the Mariacristina Crosti and Marialucia Sarnicola.

Statement: During the preparation of this work the authors used [ChatGPT] in order to assist with grammar checking. After using this tool/service, the authors reviewed and edited the content as needed and take full responsibility for the content of the publication.

Appendix A. Supplementary data

Supplementary data to this article can be found online at https://doi.org/10.1016/j.clim.2026.110676.

Data availability

Data will be made available on request.

References

[1] S. Jung, et al., The generation of stem cell-like memory cells early after BNT162b2 vaccination is associated with durability of memory CD8+ T cell responses, Cell Rep. 40 (2022) 111138.
[2] G. Guerrera, et al., BNT162b2 vaccination induces durable SARS-CoV-2-specific T cells with a stem cell memory phenotype, Sci. Immunol. 6 (2021) eabl5344.
[3] S.A. Fuertes Marraco, et al., Long-lasting stem cell-like memory CD8 + T cells with a naïve-like profile upon yellow fever vaccination, Sci. Transl. Med. 7 (2015) 282ra48.
[4] L. Gattinoni, et al., A human memory T cell subset with stem cell–like properties, Nat. Med. 17 (10) (2011) 1290–1297.
[5] M.E. Vakili, et al., Lower frequency of T stem cell memory (TSCM) cells in hepatitis B vaccine nonresponders, Immunol. Res. 70 (2022) 469–480.
[6] C.W. Cai, I. Sereti, Residual immune dysfunction under antiretroviral therapy, Semin. Immunol. 51 (2021) 101471.
[7] C. Fenwick, et al., T-cell exhaustion in HIV infection, Immunol. Rev. 292 (2019) 149–163.
[8] C. Fritzsche, L. Bergmann, M. Loebermann, A. Glass, E.C. Reisinger, Immune response to hepatitis a vaccine in patients with HIV, Vaccine 37 (2019) 2278–2283.
[9] D. Hillus, et al., Safety and effectiveness of MVA-BN vaccination against mpox in at-risk individuals in Germany (SEMVAc and TEMVAc): a combined prospective and retrospective cohort study, Lancet Infect. Dis. 25 (2025) 775–787.
[10] C.M. Wilson, et al., Serologic response to hepatitis B vaccine in HIV infected and high-risk HIV uninfected adolescents in the REACH cohort. Reaching for excellence in adolescent care and health, J. Adolesc. Health 29 (2001) 123–129.
[11] E. Motta, et al., Immunogenicity and reactogenicity of yellow fever vaccine in people with HIV, AIDS 37 (2023) 2319–2329.
[12] A. Weinberg, et al., Persistence of memory B-cell and T-cell responses to the quadrivalent HPV vaccine in HIV-infected children, AIDS 32 (2018) 851–860.
[13] P. Tebas, et al., Poor immunogenicity of the H1N1 2009 vaccine in well controlled HIV-infected individuals, AIDS 24 (2010) 2187–2192.
[14] J.M. Tesoriero, et al., COVID-19 outcomes among persons living with or without diagnosed HIV infection in New York state, JAMA Netw. Open 4 (2021) e2037069.
[15] M.M. Mellor, et al., Risk of adverse coronavirus disease 2019 outcomes for people living with HIV, AIDS 35 (2021) F1–F10.
[16] A. Antinori, et al., Humoral and cellular immune response elicited by mRNA vaccination against severe acute respiratory syndrome coronavirus 2 (SARS-CoV-2) in people living with human immunodeficiency virus receiving antiretroviral therapy based on current CD4 T-lymphocyte count, Clin. Infect. Dis. 75 (2022) e552–e563.
[17] S. Benet, et al., Limited humoral and specific T-cell responses after SARS-CoV-2 vaccination in PWH with poor immune reconstitution, J. Infect. Dis. 226 (2022) 1913–1923.
[18] J. Frater, et al., Safety and immunogenicity of the ChAdOx1 nCoV-19 (AZD1222) vaccine against SARS-CoV-2 in HIV infection: a single-arm substudy of a phase 2/3 clinical trial, Lancet HIV 8 (2021) e474–e485.
[19] L. Nault, et al., Covid-19 vaccine immunogenicity in people living with HIV-1, Vaccine 40 (2022) 3633–3637.
[20] M. Sisteré-Oró, et al., Anti-SARS-COV-2 specific immunity in HIV immunological non-responders after mRNA-based COVID-19 vaccination, Front. Immunol. 13 (2022) 994173.
[21] S.B. Coburn, et al., Analysis of post vaccination breakthrough COVID-19 infections among adults with HIV in the United States, JAMA Netw. Open 5 (2022) e2215934.
[22] J. Sun, et al., Association between immune dysfunction and COVID-19 breakthrough infection after SARS-CoV-2 vaccination in the US, JAMA Intern. Med. 182 (2022) 153–162.
[23] T. Sokoya, H.C. Steel, M. Nieuwoudt, T.M. Rossouw, HIV as a cause of immune activation and immunosenescence, Mediat. Inflamm. 2017 (2017) 6825493.
[24] S. Moir, T.-W. Chun, A.S. Fauci, Pathogenic mechanisms of HIV disease, Annu. Rev. Pathol. 6 (2011) 223–248.
[25] M. D'Souza, et al., Programmed death 1 expression on HIV-specific CD4+ T cells is driven by viral replication and associated with T cell dysfunction, J. Immunol. 179 (2007) 1979–1987.
[26] R.B. Jones, et al., Tim-3 expression defines a novel population of dysfunctional T cells with highly elevated frequencies in progressive HIV-1 infection, J. Exp. Med. 205 (2008) 2763.
[27] D.E. Kaufmann, et al., Upregulation of CTLA-4 by HIV-specific CD4+ T cells correlates with disease progression and defines a reversible immune dysfunction, Nat. Immunol. 8 (2007) 1246–1254.
[28] L. Trautmann, et al., Upregulation of PD-1 expression on HIV-specific CD8+ T cells leads to reversible immune dysfunction, Nat. Med. 12 (2006) 1198–1202.
[29] M. Roederer, et al., CD8 naive T cell counts decrease progressively in HIV-infected adults, J. Clin. Invest. 95 (1995) 2061–2066.
[30] M. Zeng, et al., Lymphoid tissue damage in HIV-1 infection depletes naïve T cells and limits T cell reconstitution after antiretroviral therapy, PLoS Pathog. 8 (2012) e1002437.
[31] K. Sakai, H. Gatanaga, H. Takata, S. Oka, M. Takiguchi, Comparison of CD4(+) T-cell subset distribution in chronically infected HIV(+) patients with various CD4 nadir counts, Microbes Infect. 12 (2010) 374–381.
[32] G. Galletti, et al., Two subsets of stem-like CD8+ memory T cell progenitors with distinct fate commitments in humans, Nat. Immunol. 21 (2020) 1552–1562.
[33] C. Gago da Graca, et al., Stem-like memory and precursors of exhausted T cells share a common progenitor defined by ID3 expression, Sci. Immunol. 10 (103) (2025) eadn1945.
[34] D. Zehn, R. Thimme, E. Lugli, G.P. de Almeida, A. Oxenius, 'Stem-like' precursors are the fount to sustain persistent CD8+ T cell responses, Nat. Immunol. 23 (2022) 836–847.
[35] A. Lombardi, et al., Anti-spike antibodies and neutralising antibody activity in people living with HIV vaccinated with COVID-19 mRNA-1273 vaccine: a prospective single-Centre cohort study, Lancet Reg. Health Eur. 13 (2022).
[36] E. Galeota, et al., Tracking the immune response profiles elicited by the BNT162b2 vaccine in COVID-19 unexperienced and experienced individuals, Clin. Immunol. 261 (2024).
[37] M. Shrotri, et al., Spike-antibody waning after second dose of BNT162b2 or ChAdOx1, Lancet 398 (2021) 385–387.
[38] K. Srivastava, et al., SARS-CoV-2-infection- and vaccine-induced antibody responses are long lasting with an initial waning phase followed by a stabilization phase, Immunity 57 (2024) 587.
[39] Z. Wang, et al., mRNA vaccine-elicited antibodies to SARS-CoV-2 and circulating variants, Nature 592 (7855) (2021) 616–622.
[40] A. Alrubayyi, et al., Characterization of humoral and SARS-CoV-2 specific T cell responses in people living with HIV, Nat. Commun. 12 (1) (2021) 1–16.
[41] E. Lugli, et al., Identification, isolation and in vitro expansion of human and nonhuman primate T stem cell memory cells, Nat. Protoc. 8 (1) (2013) 33–42.
[42] E. Lugli, V. Zanon, D. Mavilio, A. Roberto, FACS analysis of memory T lymphocytes, Methods Mol. Biol. 1514 (2017) 31–47.
[43] F. Sallusto, D. Lenig, R. Förster, M. Lipp, A. Lanzavecchia, Two subsets of memory T lymphocytes with distinct homing potentials and effector functions, Nature 401 (6754) (1999) 708–712.
[44] Y. Tian, et al., Unique phenotypes and clonal expansions of human CD4 effector memory T cells re-expressing CD45RA, Nat. Commun. 8 (2017).
[45] M. Di Mascio, et al., Naïve T-cell dynamics in human immunodeficiency virus type 1 infection: effects of highly active antiretroviral therapy provide insights into the mechanisms of naïve T-cell depletion, J. Virol. 80 (6) (2006) 2665–2674.
[46] R.J. De Boer, H. Mohri, D.D. Ho, A.S. Perelson, Turnover rates of B cells, T cells, and NK cells in simian immunodeficiency virus-infected and uninfected Rhesus macaques, J. Immunol. 170 (2003) 2479–2487.
[47] M.D. Hazenberg, et al., Persistent immune activation in HIV-1 infection is associated with progression to AIDS, AIDS 17 (2003) 1881–1888.
[48] A. Tarke, et al., SARS-CoV-2 vaccination induces immunological T cell memory able to cross-recognize variants from alpha to omicron, Cell 185 (2022) 847–859, e11.
[49] S. Desai, A. Landay, Early immune senescence in HIV disease, Curr. HIV/AIDS Rep. 7 (2010) 4–10.
[50] K.B. Lorvik, et al., Enhanced gut-homing dynamics and pronounced exhaustion of mucosal and blood CD4+ T cells in HIV-infected immunological non-responders, Front. Immunol. 12 (2021) 744155.
[51] C. Mallarino-Haeger, et al., HIV-1 DNA and immune activation levels differ for long-lived T-cells in lymph nodes, compared with peripheral blood, during antiretroviral therapy, J. Virol. 97 (2023).
[52] A.M. Miggelbrink, et al., CD4 T-cell exhaustion: does it exist and what are its roles in cancer? Clin. Cancer Res. 27 (2021) 5742–5752.
[53] E.J. Wherry, T cell exhaustion, Nat. Immunol. 12 (2011) 492–499.
[54] J.M. DeRogatis, et al., Cell-intrinsic CD38 expression sustains exhausted CD8 + T cells by regulating their survival and metabolism during chronic viral infection, J. Virol. 97 (2023).
[55] F. Díaz-Basilio, et al., The ecto-enzyme CD38 modulates CD4T cell immunometabolic responses and participates in HIV pathogenesis, J. Leukoc. Biol. 116 (2024) 440–455.

[56] Y. Huang, et al., Inhibition of CD38 enzymatic activity enhances CAR-T cell immune-therapeutic efficacy by repressing glycolytic metabolism, Cell Rep. Med. 5 (2024).
[57] L. Gattinoni, et al., Wnt Signaling Arrests Effector T Cell Differentiation and Generates CD8 + Memory Stem Cells 15, 2009.
[58] G. Scholz, et al., Modulation of mTOR Signalling triggers the formation of stem cell-like memory T cells, EBioMedicine 4 (2016) 50–61.
[59] F. Perdomo-Celis, et al., Reprogramming dysfunctional CD8+ T cells to promote properties associated with natural HIV control, J. Clin. Invest. 132 (2022).
[60] H. Kared, et al., Immunological history governs human stem cell memory CD4 heterogeneity via the Wnt signaling pathway, Nat. Commun. 11 (2020).
[61] K. Araki, et al., mTOR regulates memory CD8 T-cell differentiation, Nature 460 (2009) 108–112.
[62] G. Escobar, D. Mangani, A.C. Anderson, T cell factor 1: a master regulator of the T cell response in disease, Sci. Immunol. 5 (2020).
[63] B.C. Miller, et al., Subsets of exhausted CD8+ T cells differentially mediate tumor control and respond to checkpoint blockade, Nat. Immunol. 20 (3) (2019) 326–336.
[64] Z.L. Brumme, et al., Humoral immune responses to COVID-19 vaccination in people living with HIV receiving suppressive antiretroviral therapy, NPJ Vaccines. 7 (2022).
[65] C.T. Costiniuk, et al., COVID-19 vaccine immunogenicity in people with HIV, AIDS 37 (2023) F1–F10.
[66] A. Vergori, et al., Immunogenicity to COVID-19 mRNA vaccine third dose in people living with HIV, Nat. Commun. 13 (2022).
[67] Y. Alexandrova, et al., SARS-CoV-2 vaccine-induced T-cell response after three doses in people living with HIV on antiretroviral therapy compared to seronegative controls (CTN 328 COVAXHIV study), Viruses 15 (2023).
[68] Y.G. Pan, et al., Preservation of naive-phenotype CD4+ T cells after vaccination contributes to durable immunity, JCI Insight 11 (2024).
[69] E. Lugli, et al., Superior T memory stem cell persistence supports long-lived T cell memory, J. Clin. Invest. 123 (2013) 594–599.
[70] R. Fromentin, et al., CD4+ T cells expressing PD-1, TIGIT and LAG-3 contribute to HIV persistence during ART, PLoS Pathog. 12 (2016).
[71] S. Serrano-Villar, et al., HIV-infected individuals with low CD4/CD8 ratio despite effective antiretroviral therapy exhibit altered T cell subsets, heightened CD8+ T cell activation, and increased risk of non-AIDS morbidity and mortality, PLoS Pathog. 10 (2014) e1004078.
[72] J.D. Powell, G.M. Delgoffe, The mammalian target of rapamycin: linking T cell differentiation, function, and metabolism, Immunity 33 (2010) 301–311.
[73] H. Zeng, H. Chi, mTOR and lymphocyte metabolism, Curr. Opin. Immunol. 25 (2013) 347–355.
[74] T.L. Kissner, et al., Activation of MyD88 signaling upon staphylococcal enterotoxin binding to MHC class II molecules, PLoS One 6 (2011).
[75] S. Kurella, et al., Transcriptional modulation of TCR, notch and Wnt signaling pathways in SEB-anergized CD4+ T cells, Genes Immun. 6 (2005) 596–608.
[76] B.A. Torres, et al., Superantigen enhancement of specific immunity: antibody production and signaling pathways, J. Immunol. 169 (2002) 2907–2914.
[77] I.R. Ferrer, et al., Rapamycin augments pathogen-specific but not graft-reactive CD8+ T cell responses, J. Immunol. 185 (2010).
[78] R.J. Salmond, mTOR regulation of glycolytic metabolism in T cells, Front. Cell Dev. Biol. 6 (2018) 122.
[79] E. Touizer, et al., Attenuated humoral responses in HIV after SARS-CoV-2 vaccination linked to B cell defects and altered immune profiles, iScience 20 (2023) 26.
[80] Y.Y. Tang, et al., Effects of glycogen synthase kinase-3β inhibitor TWS119 on proliferation and cytokine production of TILs from human lung cancer, J. Immunother. 41 (2018) 319–328.
[81] L. Gattinoni, et al., T memory stem cells in health and disease, Nat. Med. 6 (2017) 23.